HYDROTHERMAL SYNTHESIS AND CHARACTERIZATION OF TUNGSTEN OXIDE CONTAINING ORGANIC-INORGANIC HYBRID MATERIAL

A Thesis Submitted to
The Graduate School of Engineering and Sciences of
İzmir Institute of Technology
in Partial Fulfillment of the Requirements for the Degree of

MASTER OF SCIENCE

in Chemistry

by
Langson CHILUFYA

July 2019
İZMİR

We approve the thesis of **Langson CHILUFYA**

Examining Committee Members:

Prof. Dr. Mehtap EANES
Department of Chemistry, İzmir Institute of Technology

Doç. Dr. Mustafa EMRULLAHOĞLU
Department of Chemistry, İzmir Institute of Technology

Prof. Dr. Funda DEMİRHAN
Department of Chemistry, Celal Bayar University

12th July, 2019

Prof. Dr. Mehtap EANES
Supervisor, Department of Chemistry
İzmir Institute of Technology

Prof. Dr. Ahmet E. EROĞLU
Head of the Department of Chemistry

Prof. Dr. Aysun SOFUOĞLU
Dean of the Graduate School of
Engineering and Sciences

ACKNOWLEDGMENTS

Let me take this opportunity to extend my heartfelt thanks to my research supervisor and indeed great mentor Professor. Dr. Mehtap Eanes for his guidance from the beginning of the research to its conclusion. Much appreciated for introducing me to the field of polyoxometalates in inorganic chemistry which have come to love so much.

My thanks also goes to Assoc. Prof. Dr. Mustafa Emrullahoğlu for critical important support in all organic synthesis and the use of his lab. I would also like to thank Assoc. Prof. Dr. Yasar Akdoğan for the tremendous help with supply of organic compounds.

I also wish to thank Ms. Özlem Ece for assistance with many aspects of this project in the laboratory and instrumentation applications. I am also grateful to Ms. Suay Dartar and Mr. Beraat Kaya for help with most of organic part and experimental purification procedures.

Many thanks to the Center of Materials Research (İYTE-MAM) researches for Powder X-ray Diffraction, Scanning Electron Microscope (SEM-EDX) and thermogravimetric analyses and all the support staff in department of chemistry at IZTECH.

I would like to express my sincere gratitude to the Turkish government through the Presidency for Turks Abroad and Related Communities for the scholarship of funding my studies and my stay in Turkey.

I am also highly indebted to the Departments of Chemistry of the University of Zambia for according me study leave and this opportunity to come and pursue my masters' degree in Turkey.

Next, I wish to express my thanks to all my friends I have made during my stay in İzmir, Turkey. You guys have been amazing and made me feel nice to call Turkey as my second home.

Lastly, but not least, I wish to express my gratitude to my Parents and my three sisters back home in Zambia. Without your emotional support, love and encouragement, this work would not have been done.

Wishing you all the best in all of your endeavors. May Jehovah God blessings be upon you all.

ABSTRACT

HYDROTHERMAL SYNTHESIS AND CHARACTERIZATION TUNGSTEN OXIDE CONTAINING ORGANIC-INORGANIC HYBRID MATERIAL

Importance and a wide area of applications of solid-state oxides are well known. Metal oxides crystallize in wide variety but simple structures. Lately general opinion is that piezoelectric, ferromagnetic and catalytic properties of simple oxide structures will be improved if the metal oxides could have more complicated and detailed crystal structures. Therefore, research interest increased towards synthesizing complicated crystal structures. One of the methods to increase the complexity of the structure is the modification of inorganic oxides with organic ligands to synthesize complex hybrid materials.

There are a great number of organic-inorganic hybrid materials with Keggin or Lindqvist Polyoxometalates structure containing Molybdenum and Tungsten. Usually Obtaining multifunctional hybrid materials, mostly requires grafting an organic functionalized group into the lacunary Keggin structures $[XM_{11}O_{39}]^{(n+4)-}$. Only Tungsten containing polyoxometalates can form a stable lacunary Keggin structures. A Lindqvist structures $[M_6O_{19}]^{2-}$ can also self-assemble with organic dyes to form a stable hybrid materials which have important applications.

These polyoxotungstates, as an inorganic building blocks, were combined with organic compounds to obtain organic-inorganic hybrid materials. The carboxylic acid functionalized organotin grafted lacunary Keggin structure was coupled with different amines using N, N'-dicyclohexylcarbodiimide (DCC). Another hybrid material was formed by the association of the Lindqvist POM with phosphine based BODIPY derivative dye. The synthesized compounds were all characterized by SEM, FT-IR, TGA and Powder XRD. Since one of the organic moiety use was a BODIPY-type organic dye, the fluorescence properties of these newly synthesized compounds were investigated.

ÖZET

TUNGSTEN OKSİT İÇEREN ORGANİK-İNORGANİK MELEZ MALZEMELERİN HİDROTERMAL SENTEZİ VE KARAKTERİZASYONU

Katı-hal oksitlerinin önemi ve geniş uygulama alanları olduğu bilinmektedir. Metal oksitler çok çeşitli şekilde kristallenmekte olup aynı zamanda basit yapılara da sahiplerdir. Son zamanlarda metal oksitlerin daha karmaşık ve detaylı kristal yapılara sahip olduklarında basit oksit yapıların pizoelektrik, ferromanyetik ve katalitik özelliklerinin geliştirilebileceği genel bir kanıdır. Bu sebeple, araştırmalar karmaşık kristal yapılara yoğunlaşmıştır. Yapıların karmaşıklığını arttıran yöntemlerden biri , anorganik oksitler ile organik ligandları birleştirerek karmaşık melez malzemeler sentezlemektir.

Molibden ve tungsten içeren Keggin ve Lindqvist polioksometalleri ile oluşturulan organik-anorganik melez malzemelerin sayısı oldukça fazladır. Genellikle çok fonksiyonlu melez malzemeler elde edebilmek için organic grup içeren tamamlanmamış $[XM_{11}O_{39}]^{(n+4)-}$ Keggin yapıları gerekmektedir. Yalnızca tungsten içeren polioksometaller kararlı tamamlanmamış Keggin yapıları oluşturabilmektedir. $[M_6O_{19}]^{2-}$ Lindqvist yapıları ise organik boyalarla kararlı melez malzemeler oluşturmaktadırlar.

Organik-anorganik melez malzemeler elde etmek için polioksotungstenler, anorganik yapı taşı olarak organik bileşiklerle biraraya getirilmiştir. Karboksilik asit fonksiyonlu organotin içeren tamamlanmamış Keggin yapısı, N, N'-disikloheksilkarbodiimit (DCC) kullanılarak oluşturulan farklı aminlerle birleştirilmiştir. Bir diğer melez malzeme de Lindqvist POM ile fosfin içeren BODIPY türevi boyanın birleştirilmesiyle oluşturulmuştur. Sentezlenen bileşikler, SEM, FT-IR, TGA ve Toz-XRD yöntemleriyle karakterize edilmiştir. BODIPY türü organik boya kullanımından dolayı sentezlenen yeni malzemelerin floresans özellikleri de incelenmişti.

TABLE OF CONTENTS

LIST OF FIGURES.....viii

LIST OF TABLES.....x

CHAPTER 1. INTRODUCTION 1

1.1. Inorganic-Organic Hybrids 1

1.2. Polyoxometalates 4

1.2.1. Keggin POM 6

1.2.2. Lindqvist POM 9

1.3. Polyoxometalate-Based Inorganic–Organic Hybrids.....10

1.3.1. Polyoxometalates Functionalized Hybrids 11

1.3.2. Polyoxometalate Non-Covalent Linked Hybrids.....17

1.4. BODIPY 17

1.5 Fluorescence Properties 20

1.5. Hydrothermal Synthesis.....23

1.6.1. Water as a Solvent 24

1.6.2 Hydrothermal Synthesis for POM-Organic Hybrid Materials.....26

1.6. Motivation of the Project 27

CHAPTER 2. CHARACTERISTIC TECHNIQUES 29

2.1. Microscopic Technique.....29

2.1.1. Optical Microscopy.....29

2.1.2. Scanning Electron Microscope (SEM) 30

2.2. Diffraction Techniques 31

2.2.1. X ray Powder Crystal Diffraction.....33

2.3. Spectroscopic Techniques.....34

2.3.1. Fourier-Transform Infrared Spectroscopy (FT-IR) 34

2.3.2. Proton Nuclear Magnetic Resonance Spectroscopy (^{1}H NMR) 35

2.3.3. Fluorescence Emission 37

2.4. Thermogravimetric Analysis 38

CHAPTER 3. EXPERIMENTAL 40
3.1. Reaction Autoclaves 40
3.2. Materials 41
3.3. Preparation of Keggin-Amide Hybrids 41
3.3.1. Synthesis of Mono-Lacunary Keggin $K_7[PW_{11}O_{39}].14H_2O$ 42
3.3.2. Synthesis and Characterization of $Cl_3SnCH_2CH_2COOH$ 42
3.3.3. Synthesis of $TBA_4[PW_{11}O_{39}SnCH_2CH_2COOH]$ 42
3.3.4. Synthesis of $TBA_4[PW_{11}O_{39}SnCH_2CH_2CONHR]$ 43
3.4. Synthesis of Lindqvist POM-BODIPY Hybrid 44
3.4.1. Synthesis of Lindqvist POM ($Na_2W_6O_{19}$) 45
3.4.2. Hydrothermal Synthesis of Lindqvist POM-BODIPY Hybrid 45

CHAPTER 4. RESULTS AND DISCUSSION 46
4.1. Keggin-Amine Hybrids 47
4.2. Lindqvist POM-BODIPY Hybrid 58

CHAPTER 5. CONCLUSION 63

REFERENCES 64

LIST OF FIGURES

Figure **Page**

Figure 1.1. The interactions of inorganic-organic hybrids 3

Figure 1.2. Polyhedral representation of common POMs 5

Figure 1.3. Polyhedral representation of the Keggin structure 7

Figure 1.4. Polyhedral representation of the five rotational isomers of the Keggin anion. The rotated M_3O_{13} groups are highlighted in green.....7

Figure 1.5. Ball and stick (left) and polyhedral representation (right) for the α-$[XM_{12}O_{40}]^{n-}$ Keggin anion showing the different classification of the oxygen atoms.....8

Figure 1.6. Structure of saturated Keggin anion (a) and lacunary Keggin anion (b).....8

Figure 1.7. Ball and stick (left) and polyhedral representation (right) for the Lindqvist $[M_6O_{19}]^{n-}$ 10

Figure 1.8. POM-Dye hybrid 10

Figure 1.9. A hybrid compound with a transition metal (Cu) linking the POM and organic moiety 11

Figure 1.10. Schematic representation of the different synthetic routes for the designof covalent POM-based organic–inorganic hybrids. Path (i): direct functionalization, paths (ii, iii): post-functionalization. The Lacunary POM is represented in blue, while the anchoring tether is lilac and the added functional moiety (F) is beige. 13

Figure 1.11. POM functionaliztion of Mono Lacunary Keggin and Dawson POMs and coupling of the dye by Sinogashira reaction 14

Figure 1.12. Stepwise functionalization of Organotin lacunary Keggin POM 16

Figure 1.13. The Amidation reaction of iso-butyl POSS and Polyoxometalates in EEDQ 16

Figure 1.14. BODIPY Core structure.....18

Figure 1.15. Applications of BODIPY derivative.....19

Figure 1.16. representation of the anionic unit in BODIPY–POM–BODIPY 20

Figure 1.17. Structure of POMs and toym ligand Emission spectra of toym ligand, 1 and 2 at RT 21

Figure **Page**

Figure 1.18. The structure POM-Pyrene systems showing and the Absorption spectra: 1-ethynylpyrene (black), TBA-K[Pyr] (blue) and TBA-D[Pyr] (red).....23
Figure 1.19. Different interaction linkages between a Keggin POM and an organic Pyridine 27
Figure 2.1. Electron beam scanning of surface 30
Figure 2.2. Generation of Characteristic X-rays 32
Figure 2.3. Diffraction of X rays.....32
Figure 2.4. The continuous wave spectrometer.....35
Figure 2.5. Fluorescence spectroscopy 37
Figure 3.1. Steel autoclave and Teflon vessel. 40
Figure 3.2. Steel autoclave placed in oven.....41
Figure 4.1. FT-IR spectrum of $K_7[PW_{11}O_{39}].14H_2O$ 47
Figure 4.2. SEM images of $K_7[PW_{11}O_{39}].14H_2O$ 48
Figure 4.3. SEM/EDX spectrum and table of results of $K_7[PW_{11}O_{39}].14H_2O$ 48
Figure 4.4. Powder XRD spectrum of $K_7[PW_{11}O_{39}].14H_2O$.....49
Figure 4.5. FT-IR spectrum of Sn [COOH] 50
Figure 4.6. The IR spectrum of TBA-K_{Sn}[COOH] 51
Figure 4.7. The FT-IR of TBA [K_{Sn}CO-Ph] 52
Figure 4.8. The TGA curve of TBA [K_{Sn}CO-Ph]…….…….53
Figure 4.9. The obtained Powder XRD of TBA [K_{Sn}CO-Ph]…….……...54
Figure 4.10. The FT-IR of TBA [K_{Sn}CO-Leu] 55
Figure 4.11. The TGA curve of TBA [K_{Sn}CO-Leu]……..…….56
Figure 4.12. The obtained Powder XRD of TBA [K_{Sn}CO-Leu]…….……...57
Figure 4.13. The SEM of crystals of $Na_2W_6O_{19}$.....…...58
Figure 4.14. The FT-IR spectrum of the Lindqvist POM [W_6O_{19}]……59
Figure 4.15. Powder XRD of $Na_2W_6O_{19}$.....60
Figure 4.16. The IR spectrum of Lindqvist POM-Dye hybrid.....61
Figure 4.17. The TGA Curve of the Lindqvist POM-BODIPY hybrid……..62
Figure 4.18. Powder XRD of Lindqvist POM-BODIPY dye hybrid…….63

LIST OF TABLES

Table **Page**

Table 3.1: Organic moiety used with amine group 44

Table 4.1: The EDX results of $K_7[W_{11}O_{19}].14H_2O$ 49

Table 4.2: The TGA weight losses with temperature of TBA [K_{Sn}CO-Ph] 54

Table 4.3: The TGA weight losses with temperature of TBA [K_{Sn}CO-Ph] 57

Table 4.4: The EDX results of $Na_2W_6O_{19}$ 58

Table 4.5: The characteristic IR peaks spectrum of: $Na_2W_6O_{19}$, dye and POM-Dye hybrid 60

Table 4.6: The weight loss with temperature of Lindqvist POM-BODIPY hybrid 62

CHAPTER 1

INTRODUCTION

Solid state chemistry is one of the most important branches in inorganic chemistry which has a vast area of applications. Solid materials can readily combined with other materials to make complicated crystal structures with improved properties. One way this is done, is by reacting an inorganic solid oxide with an organic moiety, to make a hybrid materials. There are a number of different ways to synthesize these inorganic-organic hybrids. One most popular method used to prepare them is the hydrothermal method (West, 2014).

The introduction of organic groups onto Polyoxometalates (POM) has proved to be one efficient way to significantly increase the number of inorganic-organic hybrid compounds. Moreover, some of the new hybrid synthesized from these combination have been known to have more improved properties than their individual component (Frontera, 2016). For instance, the improved property is observed in the development of POM–Dye interactions. The formation of these kind of hybrids has enabled most dyes to tackle the quenching process or enhancing the fluorescence properties of such hybrid systems (Matt, 2012).

1.1. Inorganic-Organic Hybrids

Inorganic-organic hybrid materials are formed by the association of inorganic and organic components. These materials represent the interaction between the two major branches of chemistry that is organic and inorganic chemistry. (Hagrman et al, 1999) There has been rapid progress in the past few years in exploring these organic-inorganic hybrid materials. This has been necessitated by the elaborate wide field of application of these intriguing variety of hybrids. Some notable strides of major applications are in field such as catalysis, medicine, electrical, optical, and magnetic materials. (Zhang, 2016)

Despite being in existence for centuries since their successful mixing, the concept of “organic-inorganic” hybrid materials exploded only very recently with the birth of soft

inorganic chemistry processes called the “Chimie Douce”. This process used mild synthetic conditions which allowed versatile access to chemically design an organic-inorganic hybrid materials. (Sanchez, 2001) Basically, these hybrid compounds are available in both non-crystalline and crystalline materials. The crystalline hybrid are mostly prepared by reactions at room temperature, reflux conditions and under hydrothermal conditions (Zhang, 2016).

The synthesis of novel organic inorganic hybrids has led to the development of multifunctional hybrid materials. The combination of inorganic and organic materials makes the hybrids both have the properties of them. In these hybrids the functions of both organic and inorganic components are perfectly maintained. Furthermore, the hybrid materials also creates synergistic effects that make the comprehensive properties and performances much more improved in comparison to their unique properties of each component (Yang, 2017).

Different supramolecular arrangements have been made because of this synergism between organic and inorganic components. The advanced properties of these hybrid materials does not only give the sum of the individual contributions, but the favorably combined role of their inner interfaces is predominant (Fatma, 2017). The nature of the interface between the organic and the inorganic components derives the interaction within such organic-inorganic hybrid materials (Cronin, 2010). The combination of these often dissimilar properties into one hybrid material is the most noticeable advantage of most inorganic-organic hybrids (Hagrman et al, 1999). Therefore, in research activities of synthesizing these hybrids materials, the synergistic effect carrying properties of them has been considered.

In general, the classification of these hybrids is based on the interaction between the inorganic and organic component. To this respect the nature of these linkages helps to classify these hybrids. These hybrids are divide them into two distinct classes depending on the nature of the bonds between organic and inorganic components (Fatma, 2017). These classification are well known to be:

- **In Class I** hybrid materials, the organic and inorganic components are linked by very weak bond. These linkage bonds are called the Non-covalent interactions. Good examples of these are the Van der Waals interactions, hydrogen bonding, or electrostatic interaction. They are major driving forces of self-assembly in these hybrids.

- **In Class II** hybrid materials, the strong covalent interaction bonds links together the organic and inorganic. These makes these hybrids to be very strong and stable than class 1 hybrids.

The strength of these interactions has made it easy to categorize some complicated wide variety of systems containing inorganic-organic hybrid (Frontera, 2012). It can therefore be deduced that the covalent based mode forms very stable hybrids than those based on non-covalent forms. Figure 1.1 gives an overview of the strength of these categories of interactions of inorganic-organic hybrids.

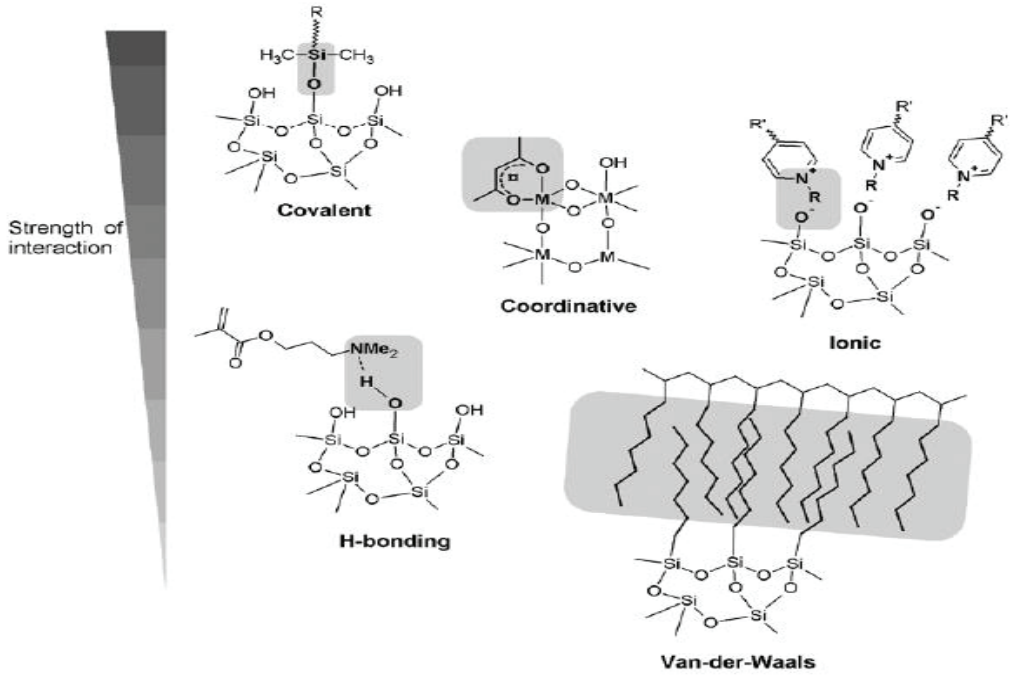

Figure 1.1. The interactions of inorganic-organic hybrids (Source: Hagrman, 1999).

A wide range of organic and inorganic components have been used in synthesis of these hybrid materials. The selection of the organic component is extremely important in the process of assembling inorganic–organic hybrids. In non-covalent hybrids, the Organic component can adjust or control the nucleation and growth of the inorganic component, thereby affecting the geometry of the final structures (Hagrman et al, 1999). This control by an organic component has revealed a good interactive structural hierarchy in these materials. The incorporation of the inorganic moiety contributes to the increased complexity and functionality as one hybrid material. These features also has driven many

researchers to elaborate on synthetic and structural functional relationships for such hybrid compositions (Yang, 2017).

Nevertheless, there is still a challenge in formation of these inorganic-organic hybrid materials. One notable challenge, is to form a hybrid material that has the best properties of both moieties with elimination or reduction in their particular limitations (Fatma, 2017). One way to overcome this drawback, Polyometalates have been employed and mostly used as inorganic component in these hybrid materials. (Frontera, 2015)

1.2. Polyoxometalates

In chemistry, polyoxometalates (**POMs**) are defined as polyatomic anion that consists of three or more transition metal atoms linked together by oxygen atoms to form clusters with finite size and geometry. The transition metal oxide units are usually from Vanadium (V), Niobium (Nb), Molybdenum (Mo) and Tungsten (W) in their higher oxidation states. Besides the metal oxide units, POM clusters can encompass other elements which are called Heteroatoms. The best examples of these heteroatoms are Phosphorus (P), Silicon (Si), Arsenic (As) and Sulphur (S) in their structures (Banu, 2011).

Since the discovery of the first POM by Berzelius in 1926, there is a lot which has been done in this field. More specifically, in the last two decades, the global interest in POMs and the rate of discovery of novel species has dramatically increased. (Riyadh, 2014) The reason for this massive development has been due to many developments in instrumentation techniques and novel synthetic approaches of POMs. The advances in analytical techniques such as Single crystal XRD have made many complex POM architecture synthesized to be characterized and added to the literature every year. (Cronin, 2010). A quite big number and variant of POMs have synthesized and characterized in the past years. For instance, it has been shown that POMs are a unique family which have remarkable diverse versatile structural topologies and abundant chemical combination. In addition they are endowed with well controllable shape, size and high negative charge (Pope, 1978).

Basically, these POMs have been classified into two major groups. These groups of compounds are based upon metal-oxide building blocks (**MO_x**), where M is the addenda atom;

- First type is the isopoly anions $[M_mO_y]^{p-}$ or isopolyoxometalates, where M is transition metal cations interlinked through oxide anions to make up the framework.
- The second type is the heteropoly anions $[X_xM_mO_y]^{q-}$ or heteropolyoxometalates compounds. The heteroatom (X) which is usually of the p- or d-block elements of the periodic table is involved in the formation of metal-oxide cluster (Riyadh, 2014).

Based on this classification, the structures of the POMs have been categorized. Examples of some fundamental polyoxometalate structures are shown in Figure 1.2 below exhibiting Lindqvist, Keggin, Dawson and Anderson structures. The Lindqvist ion is an isopolyoxometalates, and the other three are hetero-polyoxometalates. The Keggin and Dawson structures have tetrahedrally coordinated hetero-atoms, such as phosphorous or silicon while Anderson structure has an octahedral central atom, such as aluminum (Cronin, 2010).

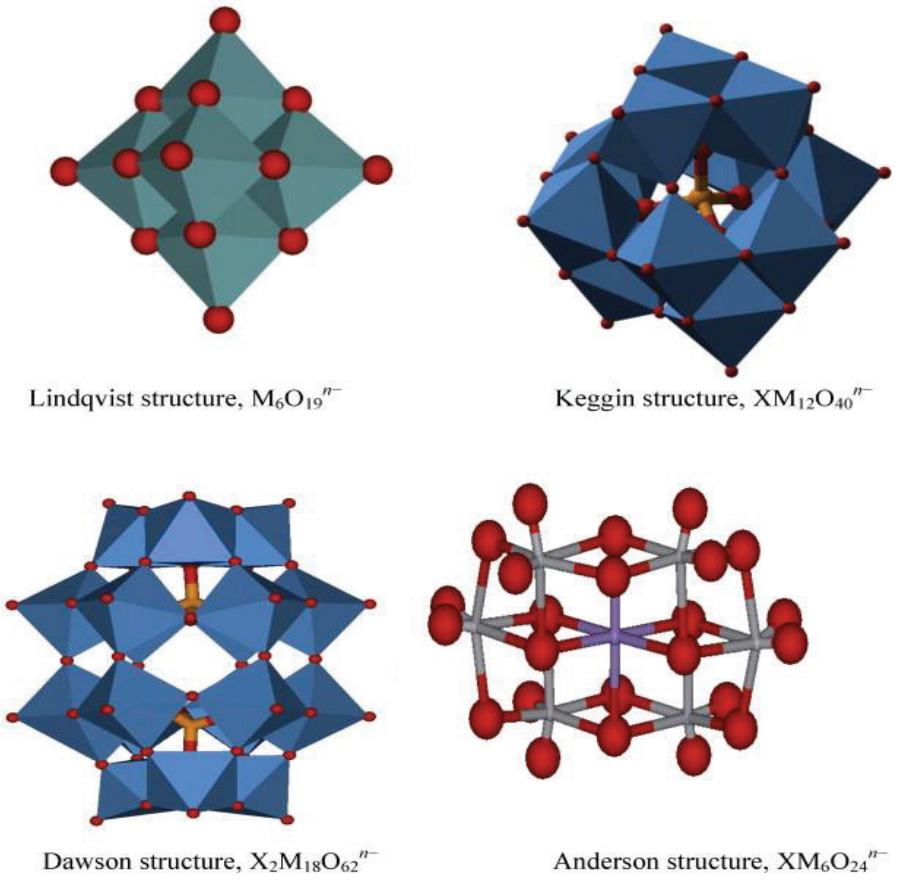

Figure 1.2. Polyhedral representation of common POMs (Source: Cronin, 2010).

POMs are a subset of metal oxide which represent a major group of inorganic clusters with abundant potential applications. These POM clusters have very unique and remarkable physical and chemical properties. Due to their intriguing and abundant topologies, POMs have reliably been utilized in the formation of new materials. (Eanes, 2015) One noticeable property is to act as a set of transferable inorganic building blocks in combination with other materials. Henceforth, because of these versatile properties, POMs have attracted a great deal of potential applications in many important fields. Some major known applications include medicine, environment, catalysis, material science, and energy and information technologies (Onen, 2011).

Polyoxotungstates (polyoxometalates with tungsten as the metal) are the best POM forms. This is due to owing to their favorable combination and the convenience of empty d-orbitals for tungsten metal-oxygen pi bonding (Wang et al, 2017).

1.2.1. Keggin POM

Keggin structures are considered as the most stable structures in POM structural chemistry. This polyanion got its name from the author who made its structural characterization in 1934 (Cronin, 2010). Among the types of POMs, the Keggin POM has been extensively used.

In these big family of POMs, the Keggin structures can made easier than any other POMs. In addition, these polyanions can easily self-assembles in acidic aqueous solution and are the most resistant structure of POMs (Wang, 2016). Furthermore, Kegging are ideal for making hybrids, because of their diverse coordination styles via terminal and bridging oxygens and suitable sizes. Other important properties are their diverse electronic, magnetic, photochemical and catalytic properties (Zhao, 2016). It is some of these interesting properties that make Keggin POM to have been vastly studied in the last decade with many applicable uses.

The Keggin polyanions have the formula $\mathbf{[}X_xM_{12}O_{40}\mathbf{]}^{(8-x)-}$ where M is mostly W or Mo and X is the heteroatom, most commonly Si or P. The Keggin structure is constituted by a central atom X, tetrahedral bonded to four oxygen atoms forming a XO_4 group. The XO_4 tetrahedron is surrounded by twelve octahedrons MO_6 that can be arranged into four groups of three octahedral units, M_3O_{13}, by edge sharing of the MO_6 units. These octahedral units bind each other through corner-shared oxygen atoms and

through the central XO_4 tetrahedron (Zhang et al, 2016). The Polyhedral representation of the Keggin structure in Figure 1.3 exhibits four groups of M_3O_{13} in four different colors and the central tetrahedron XO_4 in yellow.

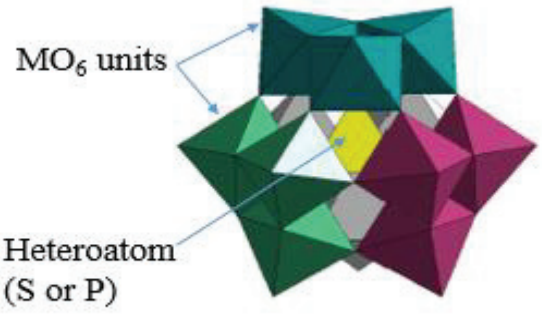

Figure 1.3. Polyhedral representation of the Keggin structure (Source: Cronin, 2010).

The Keggin anion has five geometrical isomers (Figure 1.4), resulting from a 60º rotation of a M_3O_{13} group relatively to the isomer α-Keggin anion. From the isomer α, isomers β, γ, δ and ε can be obtained by a 60º rotation of one, two, three or four groups M_3O_{13} respectively. These rotational orientations of the M_3O_{13} units lower the symmetry of the overall structure (Zhao, 2016). Among these isomers, the α-isomer is the most studied in which the metal centers are all equivalent.

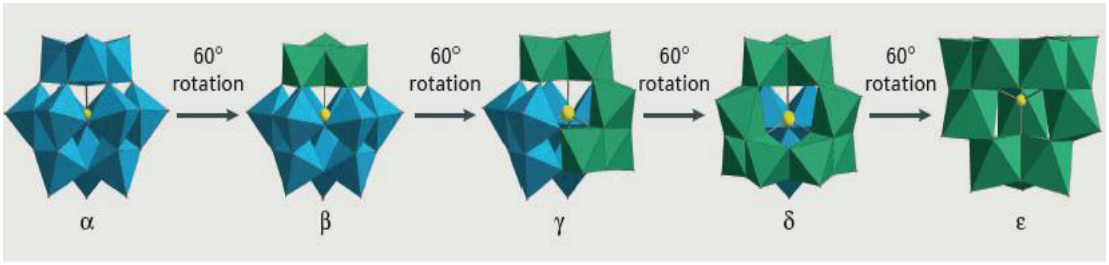

Figure 1.4. Polyhedral representation of the five rotational isomers of the Keggin anion. The rotated M_3O_{13} groups are highlighted in green. (Source: Cronin, 2010).

Among the POM types, the Keggin structure is considered to be the most stable. This is due to the strong metal-oxygen bonds present in this POM structure (Fatma, 2017). The arrangement of these bonds in a Keggin framework has been divided

according to position of the oxygen atoms in the structure. Thus an oxygen atom linked to the central atom X is designated by O_a, while those that share a corner or an edge are designated as O_b and O_c respectively and O_d represents a terminal oxygen. In Figure 1.5 shown is a schematic representation of the relative positions of the different oxygen atoms present in a POM structure using as example the Keggin anion α-$[XM_{12}O_{40}]^{n-}$ (Frontera, 2014).

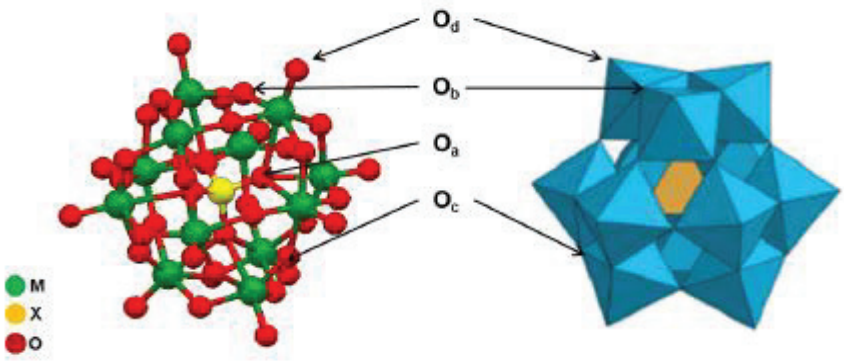

Figure 1.5. Ball and stick (left) and polyhedral representation (right) for the α$[XM_{12}O_{40}]^{n-}$Keggin anion showing the different classification o the oxygen atoms (Source: Frontera, 2014).

To create changes in the properties of the Keggin anion it is possible to obtain several lacunar structures by removing one or more MO_x octahedrons. The monolacunary anion $[XM_{11}O_{39}]^{(n+4)-}$ derives from the removal of a MO_4^+ unit that is a metal with its terminal oxygen from the saturated Keggin POM. (Yang Chu 2017) Therefore as shown in Figure 1.6, this creates a reactive vacancy site or a lacunar that need to be filled.

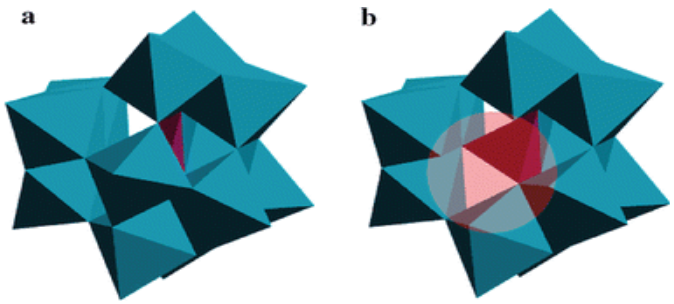

Figure 1.6**.** Structure of saturated Keggin anion (**a**) and lacunary Keggin anion (**b**) (Source: Yang, 2017).

The loss of this metal-oxygen octahedral from the saturated can be done by either alkaline or acidic hydrolysis. The preparation of all monovacant Keggin species depends on pH control. For instance, on in Polyoxotungstate with P as the heteroatom, their formation is dependent on pH in solution. The cleavage of W-O bonds resulting in loss of W octahedral at high pH. The lacunar formed has four oxygen are accessible at the surface for further reaction (Shan, 2014).

Despite their multiple negative charges, polyoxotungstates are generally poor nucleophiles. This phenomenon can be explained by the fact that their anionic charge is usually concentrated in the center of the structure (Wang et al, 2017). Therefore, the removal of a metal octahedral leads to an increased in and localization of the anionic charge in the vacancies left behind. The resulting lacunar surface oxygens have higher charges hence increased basicity and nucleophilicity than their parent complete species. The nucleophilicity properties of the oxygen atoms localized at the surface of the lacuna are increased and therefore make these oxygen atoms more reactive toward electrophilic groups (Zhao, 2016). The lacunary POM is one of the most important precursors for modification and functionalization of various novel POM-based materials (Yang Chu, 2017).

1.2.2. Lindqvist POM

Lindqvist $\mathbf{[M_6O_{19}]^{n-}}$ is an example of iso-POMs that has a metal oxide framework without the internal heteroatom. As a result, they are less stable than their hetero-POMs counterparts. (Tsunashima: 2012) However, they have some very intriguing physical properties than the hetero-polyoxometalates, such as high charges and strongly basic oxygen surfaces. This means they are attractive building blocks and can easily combine with electrophilic groups. Furthermore they can self-assemble by electrostatic interactions and hydrogen bonding (Rompel, 2018).

This type of POM has been extensively studied because of its easy preparation. The electrophilic terminal oxygen are used to react with different types of organic nucleophiles to form covalently linked hybrids (Fatma, 2017). Figure 1.7 shows both the ball and stick as well as the polyhedral representation of the POM. The bonds between the metal and oxygen forms cluster of six octahedral units with bridging oxygen (O_b) and terminal oxygen (O_t).

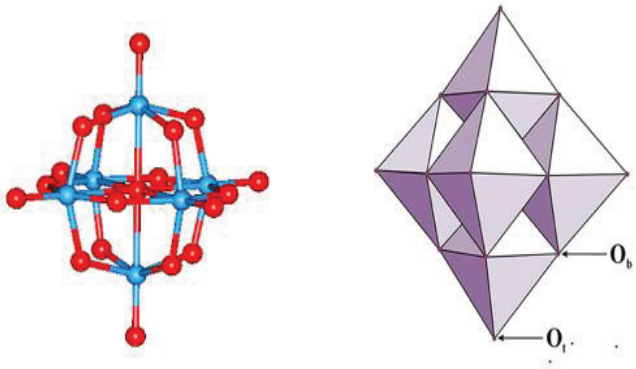

Figure 1.7. Left - Ball and stick representation. Right - polyhedral representation for the Lindqvist $[M_6O_{19}]^{n-}$ (Source: Rompel, 2018).

1.3. Polyoxometalate-Based Inorganic–Organic Hybrids

The preparation of POM-based compounds is an active field of research. In particular, the combination of POMs with organic molecules has brought about a variety of inorganic-organic hybrid compounds. Various POM based inorganic-organic hybrids have been synthesized based on different reactions and strategies. POMs as inorganic building blocks play a prominent role in facilitating the formation of these inorganic–organic hybrids (Wang, 2016). Generally, these hybrids follow the same classification of non-covalently linked and covalently linked inorganic-organic hybrids. Based on these classification, they are conveniently grouped into two main groups (Proust, 2008).

Group I: A two-component systems that depend on the combination of a POM and an organic component only (Cronin, 2013). Figure 1.8 shows the non-covalently linked hybrid material of a Lindquist POM and an organic dye.

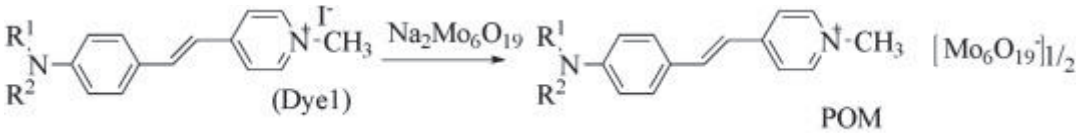

POM1 ($R^1 = R^2 =$ Ethyl)
POM2 ($R^1 = R^2 =$ n-propyl)
POM3 ($R^1 = R^2 =$ n-butyl)
POM4 ($R^1 =$ Hydroxy ethyl, $R^2 =$ Methyl)

Figure 1.8. POM-Dye hybrid (Source: Baokang et al, 2010).

There are some S/O/N-containing organic compounds which are linked with covalent bond, forming covalent interactions just between inorganic (POM) and an organic groups (Vogt, 2017). Other elements such as phosphorus, silicone or tin are covalently grafted with an organic component into the POM to form functionalized hybrids (Mialene, 2015).

Group II: Besides the POM and organic component, another element is present forming the hybrid. Most often a transition metal (Figure 1.9) is coordinated to the organic component or POM and act as a linkage between the POM and Organic component (Yang, 2017). POMs have diverse properties and coordination modes that's link to the transitional metals together with the diversity of organic linkers. This provides a great deal for the synthesis of this type of multifunctional hybrid materials. POMs and transition metals can form coordinative interaction with the organic ligands. This interaction can occur between or among them via bidentate or multidentate linkages (Fatma, 2017).

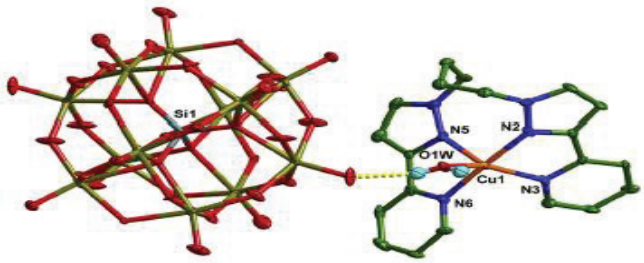

Figure 1.9. A hybrid compound with a transition metal (Cu) linking the POM and organic moiety (Source: Zhang, 2016).

1.3.1. Polyoxometalates Functionalized Hybrids

The study on functionalization of POMs has become a significant direction to develop new inorganic–organic hybrid materials which are useful. The grafting of organic groups onto the POM clusters has provided a method of fine tuning the properties of these materials towards desired applications (Hasenknopf, 2015). As earlier stated, such inorganic–organic hybrid materials will not only combine the advantages of each component, such as structural fine tuning, but also close interaction and synergistic effects of organic group and inorganic cluster (Mialene, 2015).

POM-based hybrids in early years of research, mostly relied on non-covalent approach such as an electrostatic interactions involving the exchange of the POM counter ions with organic compounds. Nevertheless, there was a lot also done in developing the covalent linked synthesis of organic POM hybrids. The covalent linked hybrids, at the moment, has many undisputable advantages as compared to non-covalent hybrids. In particular, not just strong stable interactions, the covalent hybrids have also been known to enhance the directionality and the interaction between the inorganic and organic components (Zhang et al, 2017).

It was in the last two decades that considerable attention was given to POM functionalization hybrids. The functionalization of POMs has been a great step toward the synthesis of many more complex hybrids. Much appreciated to the works of Michael Pope for laying out such a solid foundations in this progressive field (Pope, 1978).

Grafting organic moieties onto POM backbones has opened up a wide structural diversity of such hybrids that have new interesting properties such as improved long-term stability, solubility, redox behavior, spectroscopic response and biological activities of the clusters. In addition it has facilitated the synthesis of many more novel POM based functional materials (Hasenknopf, 2015).

Among the various strategies for fabricating such hybrid materials, one attractive way is to further modify the organic part of POM-based inorganic–organic hybrid molecules through common organic reactions. In this way, new derivatives with more complicated structures can be well prepared. Thus, improved methods for their synthesis have been reported that have allowed the post-functionalization of hybrid POM platforms with more-complex organic derivatives. (Proust, 2008).

For instance, Anna Proust (2013) gave an overview about the direct functionalization and post-functionalization of POMs. The POMs are grafted with a range of organic ligands and functional units as a promising strategy for the development of hybrid materials. The synthetic methodologies used to obtain these kind of hybrids are based on two approaches for POM functionalization. The first involve the introduction of organic moieties exhibiting free coordination sites into the POM. While the second one has of reactive functionalities of organic moiety which are suitable for the grafting of preformed metal complex of the POM. Figure 1.10 shows the schematic representation of the three different synthetic routes employed to synthesize covalent POM-based organic–inorganic hybrids.

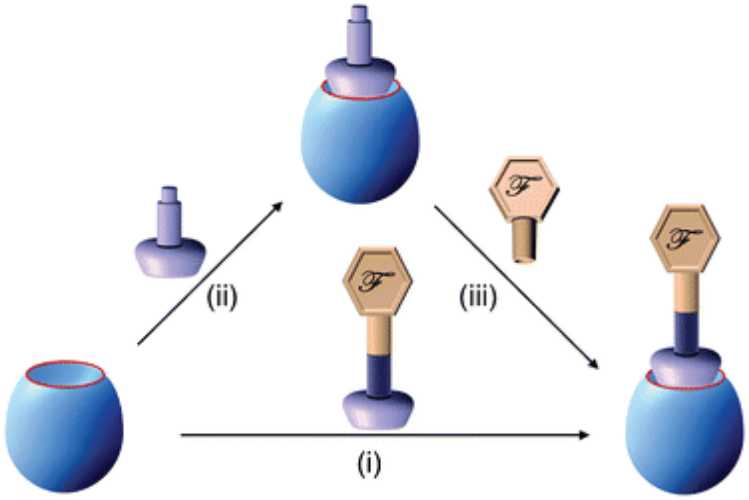

Figure 1.10. Different Paths for synthesis of covalent linked hybrids (i): direct functionalization paths (ii, iii): post-functionalization. The lacunary POM is represented in blue, while the anchoring tether is lilac and the added functional moiety (F) is beige (Source: Proust, 2012).

The first strategy is a direct functionalization where the organic moiety is pre-synthesized, providing it with an anchoring group which can be grafted into the POM. The other two are based on Post functionalization in which the anchoring group containing a specific functional group is first grafted into the POM and then reacted with the organic moiety. The advantages of this strategy are that it can preserve POMs from competitive degradation or reduction and offer greater simplicity than direct functionalization (Proust, 2013). There is still more investigation been done on synthesis of these hybrids, as each strategy has its scope and limitation (Yang, 2017).

The lacunary POMs are the most important precursors used for modification and functionalization of various novel POM-based hybrid materials. However, POM lacunary species allow convenient synthesis of various functionalized hybrids. This is because of have higher charges with increased basicity and nucleophilicity than their parent complete species. The loss of this tungsten-oxygen octahedral from the parent Keggin framework leads to an increase and localization of the anionic charge in the vacancies left behind (Hasenknopf, 2007). The presence of this vacancy in the POM cluster makes it easy to graft elements such as silicon or tin which are connected to an organic side chain. This organic side chain has functional group which makes it reactive with other organic compounds (Matt, 2011).

Direct functionalization has been applied to different type of POMs in particular the Anderson, Dawson, Lindqvist and Keggin-type POMs. The Keggin and Wells-Dawson families of heteropolyoxometalates are the two most studied types which form stable lacunas. In particular, Monolacunary Keggin $[XW_{11}O_{39}]^{n-}$ or Wells-Dawson $[X_2W_{17}O_{61}]^{m-}$ type polyoxotungstates react with organo-silanes, -germanes, and -tin to afford a variety of hybrids containing one or several functional groups (Santoni et al, 2011).

These two lacunary polyoxotungstates have special features such as high electronic density and redox properties. This is due to the high charge density and their active terminal or bridged Oxygen atoms. As can be seen below in Figure 1.10, the organosilanes forms disubstituted hybrid while the corresponding reactions with organotin give monosubstituted derivatives. The grafted organotin has a side chain which has a functional group in this case it was organo-iodine. Therefore this undergoes post functionalization of organo POM by further coupling it with a dye via Sinogashira reaction (Proust, 2012).

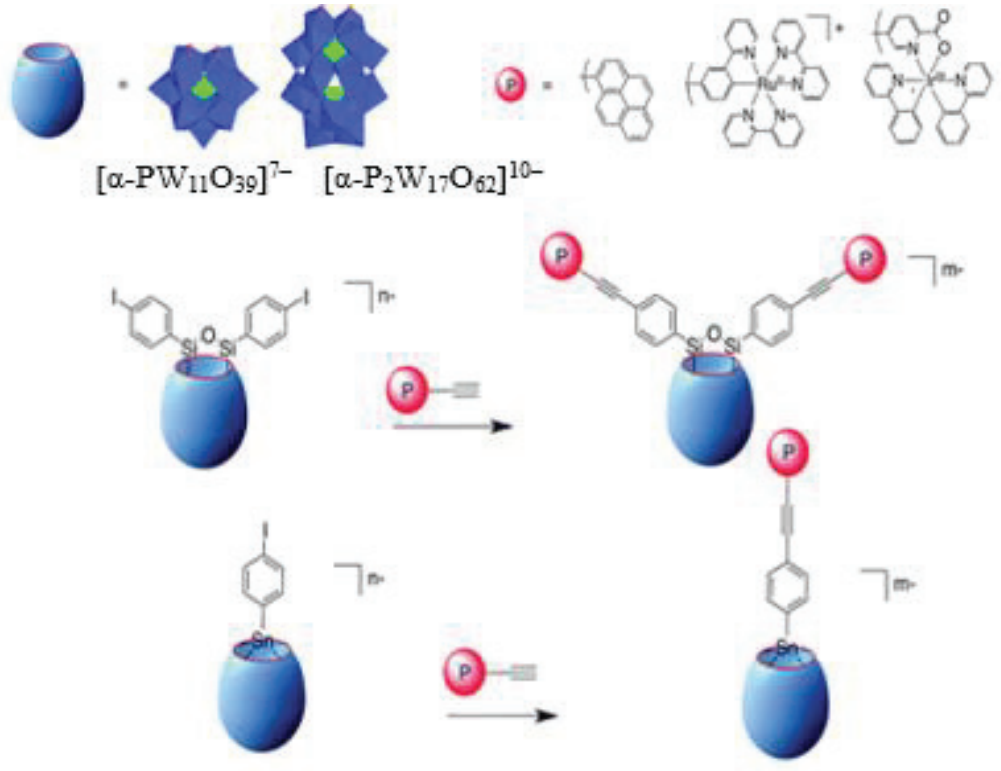

Figure 1.11. POM functionaliztion of Mono Lacunary Keggin and Dawson POMs and coupling of the dye by Sinogashira reaction (Source: Proust, 2012).

There is only a few post-functionalization reactions have been applied to POM chemistry. Because of the small number of POM platforms bearing an appropriate reactive organic moiety. In addition, the presence of the POM in the hybrid requires an adaptation of the standard protocols, which may account for the late development of such post-functionalization routes (Santon, 2014). However, the inclusion of these organic moiety has generated many new structures. Some of these species belong to the class of organotin-substituted POMs. To obtain organotin grafted POM with different R groups, one can treat different $RSnCl_3$ with lacunary POMs. This strategy though suffers from the incompatibility of the trichlorotin moiety with most organic functions, and the scarce versatility it allow (Matt, 2012).

Nevertheless, these class of polyoxoanions modified by organotin groups has drawn extensive attention because Sn (IV) fits well into the addenda sites of Keggin- and Wells–Dawson-based POM skeletons (Mialene, 2010). In addition, the enhanced hydrolytic and oxidative stability of the Sn-C bond has led to interest in broader areas of research such as medicinal chemistry of these polyoxoanions (Hasenknopf, 2013).

It's a fact that, organic ligands covalently grafted to the POM framework, are less frequently reported. This disparity is mainly due to the synthetic problems one must overcome to produce a covalent hybrid. One good example, is the multistep synthetic needed to graft an organic functionalized POM with more elaborate functions (Mialene, 2012). Therefore, the preparations of these hybrids is more appealing to many researchers.

In the last decade, many novel hybrid compounds based on Keggin clusters bearing organotin with reactive R groups have been reported (Proust, 2012). The stable Sn-C makes them to react quite easily with a variety of electrophilic groups in water or in non-aqueous solvents. In addition, the Sn-C bond allows enhanced hydrolytic and oxidative stability of these functionalized POMs. For this reason, these hybrids have found broader areas of research which include medicinal chemistry (Hasenknopf, 2013).

To prepare a functionalized POM useful as a scaffold for many applications, an organotin functionalized with carboxylic acid was grafted onto a Polyoxotungstate (Figure 1.12). A giant molecules based on organotin functionalized α-Keggin POM and Polyhedral Oligomeric Silsesquioxanes (POSS) was designed and synthesized. The functionalized Keggin with a carboxyl group combined by amidation reaction with the POSS to form this molecule (Shan, 2014).

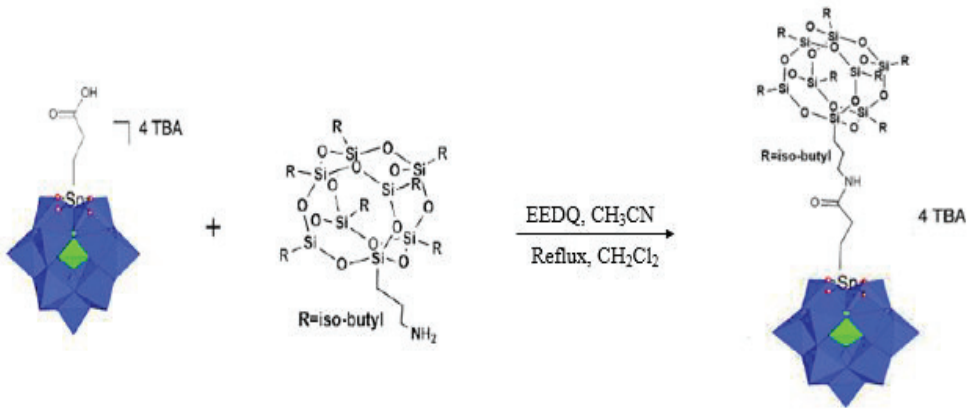

Figure 1.12. The Amidation reaction of iso-butyl POSS and Polyoxometalates in EEDQ (Source: Shan, 2014).

The use of lacunary POM carboxyl group act as a linker, with appropriate reaction conditions has enabled to attach various molecules to the carboxylic acid moiety. Many variety of organic derivatives can be added to this carboxyl side group organotin precursor by using common organic reactions. For example in Figure 1.13, the derivatized Polyoxotungstate cluster would take part in multistep reactions using the organic functionalities to create inorganic-organic hybrid materials. The stability of the Sn-C bond formed is favorable and happens without distorting the electrochemical properties of the Polyoxotungstate units. The series of reactions leads to the synthesis of one important drug used as an anti-bacterial (Hasenknopf, 2013).

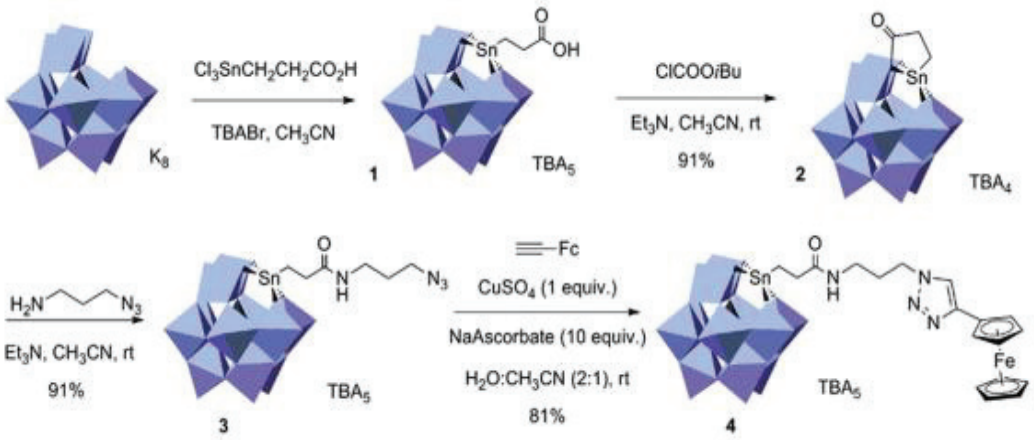

Figure 1.13. Stepwise functionalization of Organotin lacunary Keggin POM (Source: Hasenknopf, 2013)

1.3.2. Polyoxometalate Non-Covalent Linked Hybrids

In non-covalent hybrids, POMs usually have two kinds of roles they play of been a templates as well as linkages. As inorganic templates, POMs can assemble with organic cationic subunits having high negative charges and henceforth for different hybrid frameworks. On the other hand, POMs have a lot of terminal and bridging oxygen atoms which acts as linkages. The has lend them to possess diverse forms of potential coordination modes to link metal ions, including transition metals to form numerous novel structures (Cronin, 2013).

The anionic character of POMs naturally allows their association with organic counter cations in formation of complicated higher dimensional hybrids via electrostatic interactions (Zhang, 2017). The charge of the POMs is an important parameter which when combined with rigidity or flexibility of the organic ligand influences the final structure formed. The more charge of the polyanion possesses, is the priority to form strong coordination ability it has with organic ligands. Besides choosing the appropriate POM and organic moiety as the starting materials, it is always very vital to control other reaction parameters such as the pH value and time of reaction (Wang, 2017).

Although many POM-based inorganic–organic hybrids have been reported, it is still a challenging and meaningful work to obtain novel structure crystalline hybrid compounds and research their application. Typically, ligands containing amine groups have been used to synthesize many organic-inorganic hybrid compounds (Mialene, 2017). Hybrids containing dyes with attractive fluorescence properties have been explored together with their and potential applications in chemical sensors and electroluminescent displays (Mialene, 2015). BODIPY derivatives dyes have vast area of uses. One good use of BODIPY dye is having good fluorescence properties.

1.4. BODIPY

BODIPY is an abbreviation for boron-dipyrromethene which comes from the big family of Organoboron compounds with wide range of applications. The structure is composed of a dipyrromethene complexed with a disubstituted boron center, typically BF_2. The IUPAC name is 4,4-Difluoro-4-bora-3a,4a-diaza-*s*-indacene (Burgess, 2007).

The BODIPY core has a rich chemistry and variety of substitutions due to the high tolerance for pyrrole and aldehyde (or acyl chloride) starting materials. The core (Figure 1.14) carries a formal negative charge on the boron atom, and a formal positive charge on one of the nitrogen atoms (Schmitt, 2009).

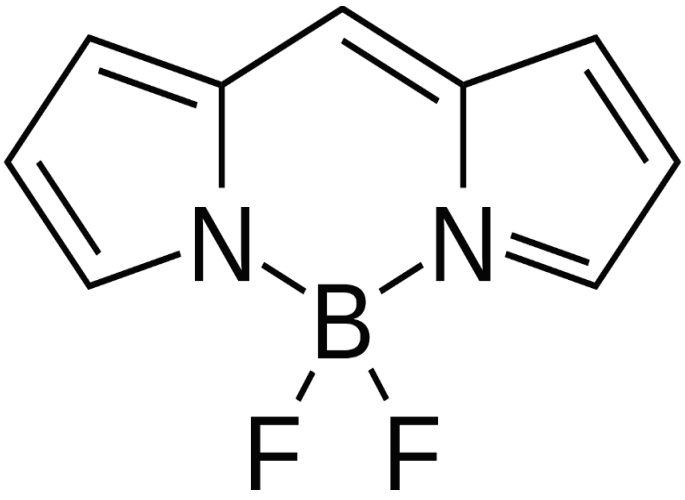

Figure 1.14. BODIPY Core structure (Source: Schmitt, 2009).

BODIPY dyes were first discovered in 1968 by Treibs and Kreuzer. The potential use of this dye then was only for biological labeling. Thereafter several new BODIPY-based dyes were designed for biological labeling which were for commercial purpose. As a consequence, BODIPY came to be known to the biochemist and biologist as a photo stable substitute for fluorescein. Many works were done on uses of BODIPY and the number of papers and patents started to escalate in the mid-1990s (Harriman, 2008). It was in 2009, when the first unsubstituted BODIPY was reported in the literature. This was because of synthetic difficulties in obtaining this compound, the pyrrole-based reactive carbons needed to be blocked from electrophilic attack (Schmitt, 2009).

BODIPY is of interest in fluorescent dyes as it tend to be a strongly UV-absorbing small molecules that emit relatively sharp fluorescence peaks with high quantum yields. The incorporation of boron into the conjugate pyrrole system makes it to have unique electronic and photophysical properties (Chai et al, 2014). Many BODIPY derivatives have been synthesized recently. These BODIPY-derivatives are the class of aromatic molecules widely used in sensors and luminescent materials (Burgess, 2007).

There are many remarkable features of BODIPY fluorophore and its derivatives. Robustness against light and chemicals, relatively high molar absorption coefficients and high fluorescence quantum yields, narrow emission bandwidths with high peak intensities, good solubility, resistance towards self-aggregation in solution, stability in physiological pH range and excitation/emission wavelengths in the visible spectral region (≥ 500 nm) could all arouse interest in these compounds (Boens et al., 2012).

Apart from this, the spectroscopic and photophysical properties of this fluorophore can be adjusted by attaching residues at the appropriate positions of BODIPY core. Among the factors that have an influence on the spectroscopic properties of BODIPY, conjugation has a substantial importance. By increasing the conjugation, there is increase in wavelength and a red shifted on the red spectrum is observed. In some instances there is a blue shift in the spectrum or loss of fluorescence properties (Cantuk, 2015). The combination of these fluorescence properties makes BODIPY to be a great fluorophores.

Most of the BODIPY derivatives emit at less than 600 nm, and mainly a handful of water-soluble derivatives have been synthesized. Thus, there is the potential that modifications to the BODIPY framework have led to compounds that can be used more effectively for different applications. (Burgess, 2007). Moreover, the fact that BODIPY could be modified according to the purpose of use is the reason why this dye has a significantly large field of application. A summary of these application fields are shown in Figure 1.15 below.

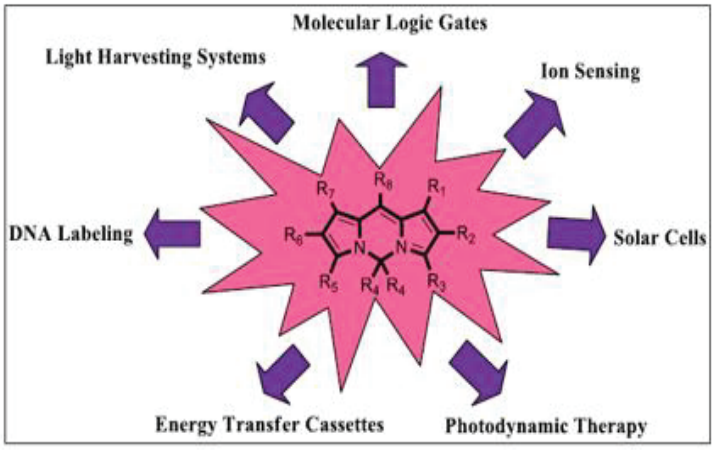

Figure 1.15. Applications of BODIPY derivatives (Source: Cantuk, 2015).

A POM and BODIPY dye hybrid has shown interesting photophysical properties. Very little has been done in literature to link these two interesting compounds in chemistry, POM and BODIPY. Mialane lab (2015) group showed how the POM can lead to electroswitched fluorescent systems through efficient energy transfer to the BODIPY unit. Figure 1.16 shows the covalent attachment of the BODIPY derivative unit with the nitrogen functionlized anderson POM.

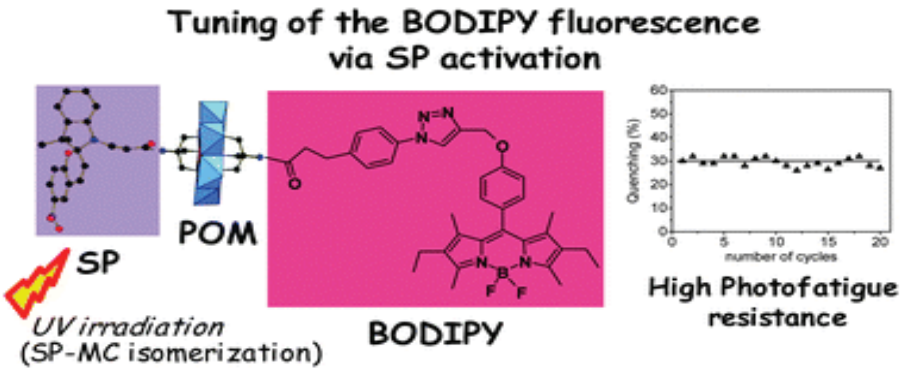

Figure 1.16. Representation of the anionic unit in BODIPY–POM–BODIPY (Source: Mialane, 2015).

The fluorescence of the BODIPY part was fine photo-controlled through the activation of the spiropyran which was grafted onto the POM. The interaction of these two significant compounds in chemistry, POMs and BODIPY entities, with massive applications has only been reported by this group.

1.5 Fluorescence Properties

In past years, inorganic–organic hybrids containing attractive fluorescence properties have been extensively studied. Generally, the inorganic moiety in the hybrid may induce the luminescent behavior by exhibiting an intense emission in respect to the luminescence spectrum of the free organic moiety (Neves, 2014). Many hybrids shows different fluorescent properties from each individual component. For instance POMs have significant electronic properties that can allow the modulation of the fluorescence of the hybrid by using electrical stimulus (Mialene, 2015).

In most POM-Dye compounds, the hybrids are assembled via electrostatic interactions. In these interactions between the cationic and anionic moieties have led to charge transfer transitions between the cationic organic dye and the polyanion (Matt et al, 2011). For covalently linked hybrids, inorganic and organic parts are connected together by covalent bond. The bond is usually much stronger than those found in non-covalently linked hybrids such as electrostatic interaction or hydrogen bonding (Fatma, 2017). This makes covalently linked hybrids more stable in most situations. In this POM-organic hybrids, the strength of these interaction gives rise to their different fluorescence (Matt, 2012).

Like shown in Figure 1.17, two different type of POMs combined with the 2,4,6-tris[1-(4-oxidroxypyridinium)-ylmethyl]-mesitylene (toym) ligand dye showed different emission peaks. With respect to the free toym ligands, the main emission peak of compound 1 was slightly blue-shifted, while the peak of compound 2 was highly red-shifted. It was concluded that, the quenching and enhancement in fluorescence intensity may be attributed to the different POM anions and the different hydrogen-bonding interactions of the two compounds (Guo, 2013).

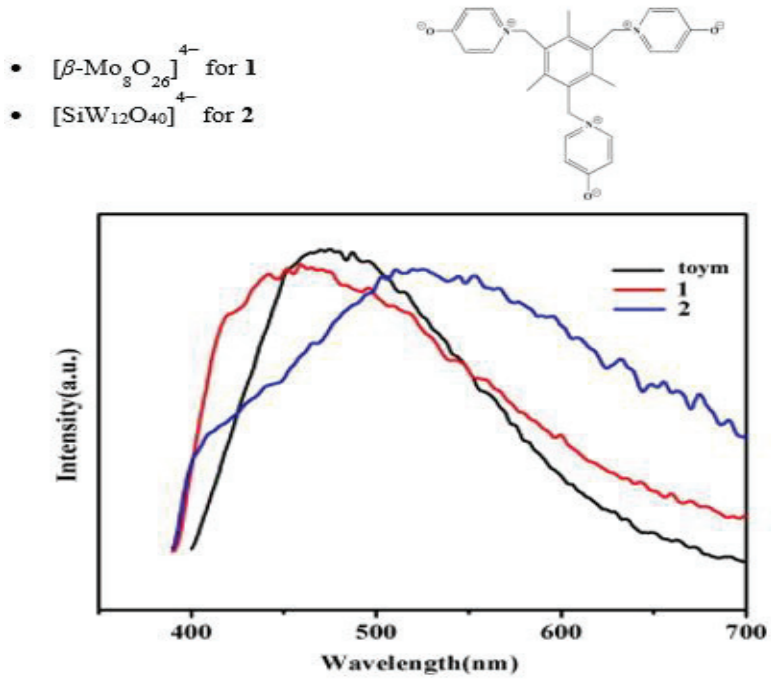

Figure 1.17. Structure of POMs and toym ligand Emission spectra of toym ligand, 1 and 2 at RT (Source: Guo, 2013).

POMs in these hybrids can either enhances or quench the fluorescence properties of the dye compared to reference by giving a shift to both the emission and excitation maximum. Most critically, the POM can act as electron reservoirs in these hybrids and store several electrons on a single cluster (Odobel, 2009). Considering this fact, has led to development of most POM-Dye materials with good photocatalytic properties. These have found potential applications as chemical sensors, and in electroluminescent displays (Yang Chu, 2017).

Fewer examples of covalently linked POM-based hybrid materials with fluorescence properties have been reported. Mainly in these hybrids, an Intramolecular charge transfer occurs between the combinations of POM and chromophore. It is also believed that the photo induced electron transfer (PET) from the Chromophore backbone to POM clusters accounts for the fluorescence. It is likely that this transfer happens through-bond electron-transfer mechanism (Matt, 2012).

However, these systems have been known to lack structural and electronic control between both fragments. Unfortunately this has resulted in the quenching of the POM-chromophore dyads. Nevertheless, these drawbacks has been overcome by damaging the destructive proton electron (PET) using molecular insulator between the POM and the dye (Fura et al, 2018).

The photophysical properties in these hybrids is remarkable. Quenching of the dye luminescence is more favored by the electron transfer to the POMs. In the case of the POM system, the lack of observation of a charge transfer state has been attributed to the poor photophysical properties of the dye. Still, the luminescence quenching of the dye is more vital in these covalent bonded hybrids than in systems where the POM and the dye are assembled via electrostatic interactions. The coupling of organometallic chromophores displaying efficient photophysical properties to the POM is currently under investigation (Matt, 2012).

The photo physical properties were investigated in POM–pyrene system (Figure 1.18). This was prepared by post functionalization of hybrid disilylated Keggin and Wells-Dawson POM platforms via Sinogashira coupling reaction. The presence of POM in these systems led to the luminescence quenching of the pyrene chromophores. These POM–pyrene hybrid systems gave a red-shift with respect to the free 1-ethynylpyrene. This was attributed to an intramolecular electron transfer from the from the pyrene moiety to the POMs (Matt et al, 2011).

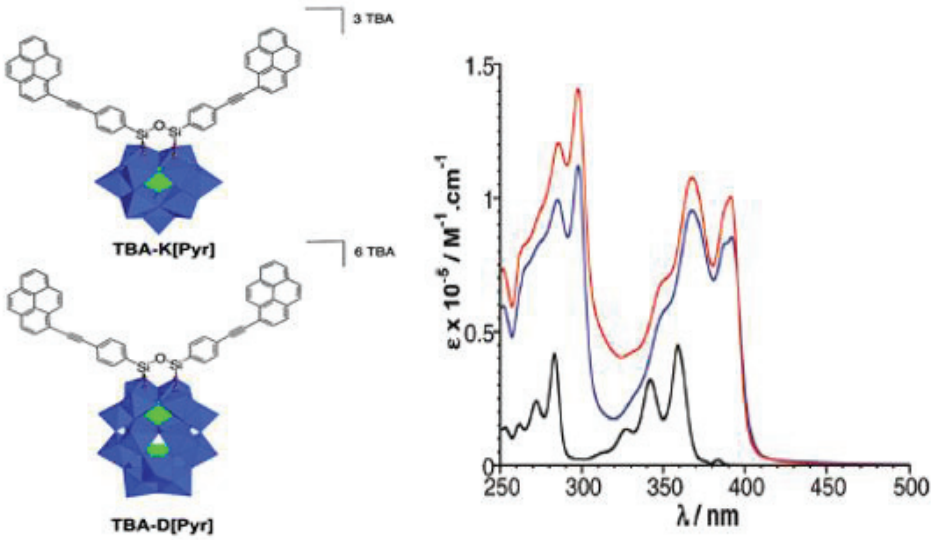

Figure 1.18. The structure POM-Pyrene systems showing and the Absorption spectra: 1-ethynylpyrene (black), TBA-K[Pyr] (blue) and TBA-D[Pyr] (red). (Source: Matt et al 2011)

The photophysical behavior of these POM pyrene systems clearly showed how the quenching process occurs by Photo-induced electron transfer from the chromophore to the POMs. Compared to the non-covalently POM-organic hybrid system assembled via electrostatic interactions, the electron transfer in fluorescence quenching is faster than in the covalently bonded hybrid. The reason could be attributed to the easy movement of electrons through the bonds. However there is still a possibility in non-covalently linked hybrids to have electron movements. This somehow shows the beneficial effect of having the covalent linkages in POM-dyes system (Proust, 2008).

1.5. Hydrothermal Synthesis

Generally, the Synthesis of inorganic-organic hybrid materials have been done using hydrothermal synthesis. This is a heterogeneous reaction which occurs in a closed system of aqueous solvents with temperature of above 100℃ and at pressures greater than 1.0atm. This is done in order to dissolve and recrystallize materials which are relatively insoluble under ordinary conditions (Byrappa, 2013). The hydrothermal technique has been most popular, gathering a lot of interest from scientists and technologists from various disciplines, particularly after the 20th century.

The term hydrothermal originated from Sir Roderick Murchison (1792-1871) the British geologist in 1845. This Geologist observed the action of water at an elevated temperature and pressure that it brought about changes in the earth's crust which lead to the formation of various rocks and minerals. The knowledge of this mineral formation in nature under elevated pressure and temperature conditions in the presence of water, led him to develop the hydrothermal technique. Years later, many earth scientists who were interested in understanding the genesis of various rocks minerals, and ore deposits. They began the hydrothermal research by studying of these natural systems and then did laboratory simulations like those conditions existing in the earth's crust (Byrappa, 2013).

Further studies were done to find new application areas of the hydrothermal technique both for science and technology. The first successful commercial application of hydrothermal technology was used for mineral extraction ore beneficiation in the nineteenth century. However, with the beginning of the synthesis of large single crystals of quartz by Nacken (1946) and zeolites by Barrer (1948), the commercial importance of the hydrothermal technique for the synthesis of these inorganic compounds was realized. The sudden demand for the large size quartz crystals during World War II forced many laboratories in Europe and North America to grow large size crystals by hydrothermal synthesis (Eral, 2006).

Nowadays, the hydrothermal technique has been widely in several branches of science and technology. In this respect, it is being rightly exploited by a large scientific community with diverse interests. This has led to many scientists to come up with several related techniques, with strong foundation from the hydrothermal technique (Byrappa, 2013). Hydrothermal processing has become a most powerful tool also for transforming various inorganic compounds and treating raw materials for functional applications (Riyadh, 2014). Water the best solvent for most chemical reactions is employed in this technique.

1.6.1. Water as a Solvent

In Nature, water is the most important solvents and its usage is environmentally beneficial. Significant properties of water are non-toxic, non-flammable, non-carcinogenic, non-mutagenic, and thermodynamically stable, and it is reasonably volatile, so easy to be filtered and removed from the product (Eanes, 2000). Furthermore,

water is a polar solvent and its polarity can be controlled by temperature and pressure (Eral, 2006). All this properties of water makes it to have more advantageous uses than over other solvents. This makes the hydrothermal technique to exhibit a great degree of flexibility and environmentally friendliness.

The properties of water under hydrothermal conditions carry the characteristics of supercritical state and it displays significant properties. Water provides a good reaction medium for easy transport, synthesis of metastable phases and the crystals growth of materials. The water is utilized under high pressure and at elevated temperature above its boiling point. At these high pressure and temperature conditions, the viscosity of water reduces. This causes the mobility of material dissolved in it to increase and diffusion process becomes easier (Banu, 2011). Furthermore, the reduced viscosity of water enhances the rates of solvent extraction of solids and good quality single crystal growth from solution. Moreover the solubility of reactants in water under these conditions can speed up the reaction between the solid particles in the closed system (Byrappa, 2013).

The differential solubility problems are minimized at hydrothermal condition of water. For this reason a variety of synthetic precursors may be introduced into the reaction system. The hydrothermal technique exploits the principle of self-assembly of the metastable solid phase from soluble precursors at relatively low temperatures (Hagrman, 1999). The materials synthesized by hydrothermal processing mostly are of a well-defined form in particle size, crystal structure, and relatively high purity even if they were made from a relatively low grade source (Ece, 2012). Otherwise in the absence of water the reactions probably occur with low yields or they may require much higher temperatures.

Hydrothermal technique is rationally designed to obtain a desired product as an elusive goal, and there are some parameters that need to be modified. These parameters include cation identity, pH value, fill volume, temperature, heating time and so on**.** They need to be manipulated in order to obtain a variety of metastable species not otherwise accessible by conventional synthetic techniques (Yang Chu, 2017)

The main disadvantage of the hydrothermal system, has been the black-box nature of the apparatus used. A closed vessel used is put in a hot oven, making it practically impossible to observe directly the crystallization processes. However, in past few years, physical chemists have made remarkable progress in this area to overcome this. They have studied of kinetics of the hydrothermal processes, which have contributed

greatly to the understanding of this technique. This has provided a solid base for designing hydrothermal synthesis and processing at much lower pressure and temperature conditions (Zhang, 2016).

1.6.2 Hydrothermal Synthesis for POM-Organic Hybrid Materials

The hydrothermal synthesis technique is a very popular strategy in the synthesis of lot of non-covalently linked POM based inorganic-organic hybrids materials (Fatma, 2017). Usually hydrothermal syntheses involving water as a solvent are conventionally carried out with temperature ranging 150-250^{O}C at autogenous pressure. These lower pressure and temperature conditions are employed in this technique are useful in the preparation of kinetically stable hybrids. Moreover, these hydrothermal conditions favor the organic structural elements to be retained without damages (Zhao, 2016).

The synthesis of hybrids is not only affected by the black-box hydrothermal environment, but also affected by the number of factors. The assembly of POM-organic hybrids have shown to be sensitive to certain synthesis conditions. As earlier stated, some parameters such as temperature, pH value, the type of starting reactants, starting concentrations and reaction time need to be monitored (Yang, 2016). For instance, it has been reported that change in pH condition may lead to the structural change in the POM-based architectures. Usually this further affected the coordinating ability of POM with the organic ligands (Frontera et al, 2014).

It is feasible to control the self-assembling of POMs-based hybrid material under hydrothermal conditions. Moreover the right choice of the organic ligand based on its intrinsic properties is a fundamental strategy for controlling and defining the role of POMs in the formation of new hybrid (Liu, 2016). A noticeable drawback is in solubility differences in the water of the organic and inorganic components. Single crystal X-ray diffraction is the main method to identify these compounds. Therefore, it is vital to obtain single crystal of good quality for the study of the hybrids. Hydrothermal technique enhances the solubility of the initial reactant species, thereby increasing the chances to obtain suitable crystals for X-ray diffraction (Zhao et al, 2015).

The structural control of the resulting POM-organic hybrid compounds by hydrothermal synthesis is still a challenging work. Despite some of these limitations, the hydrothermal technique has proven to be one of the efficient method for

the synthesis of POM-organic hybrids. Hydrothermal technique has been preferred to obtain many novel structure hybrids with retention of the organic component in the final product owing to the mild conditions of this technique (Yang, 2016).

The Zhao B (2017) published the synthesis of five Keggin polyanion-templated inorganic–organic hybrids by hydrothermal method. The versatility of this technique was shown by changing of reaction conditions. The led to formation (Figure 1.19) of four different complicated structures with retention of the structures of both the POM and organic component.

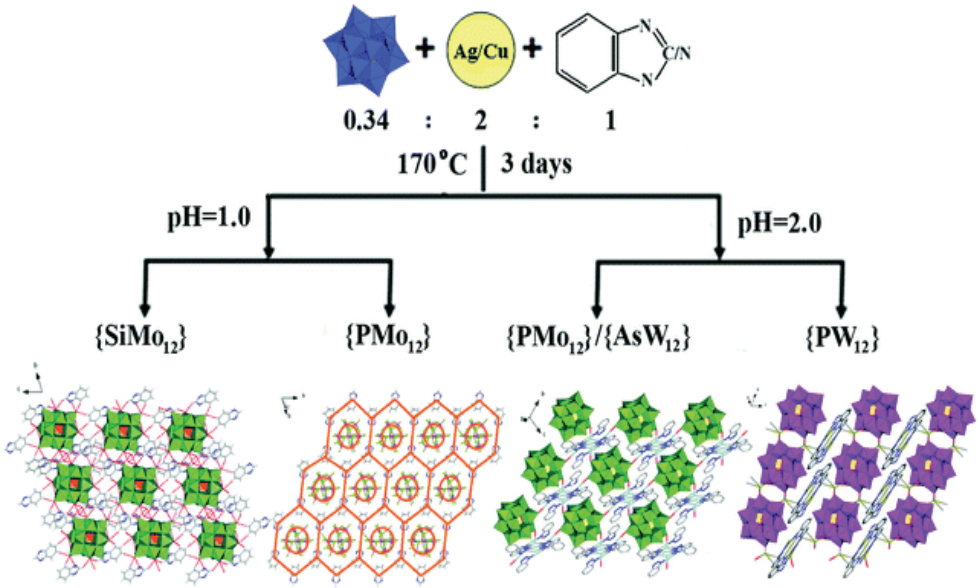

Figure 1.19. Different interaction linkages between a Keggin POM and an organic Pyridine (Source: Zhao B, 2017).

1.6. Motivation of the Project

In many publications, it is well known that POMs are extremely versatile inorganic building blocks. POMs have therefore combined with different types of organic compounds in the formation of inorganic-organic hybrids. The POM-Dye hybrids, the POM has adverse effect which changes the properties of the dye. However, hybrids containing a POM and BODIPY based dye have rarely been reported in literature. Therefore, the inorganic-organic hybrid formed from the combination of these two important compounds in chemistry with vast applications is significant.

In this project, it describes synthesis of an Inorganic-organic hybrid solid materials based on Polyoxotungstate clusters with organic derivatives by hydrothermal method. A post functionalization of an organotin lacunary Keggin POM with a carboxylic acid chain. Using appropriate reaction condition for coupling amidation, this reactive side chain can further undergo nucleophilic substitution with an organic containing an amine group.

Therefore the organic compound was coupled with Keggin POM leading to a covalently amide linked-POM conjugate. Furthermore, the Lindqvist POM was reacted with a suitable BODIPY derivative to form a non covalent hybrid. BODIPY derivative, one of the organic moieties used to make these hybrids is a good fluorophore. Therefore, the fluorescence properties of these new hybrids was investigated.

CHAPTER 2

CHARACTERISTIC TECHNIQUES

In many fields of chemistry, material science, geology and biology, detailed knowledge of the physical nature of solids is of great importance. A synthesized solid must be characterized to get its identity and further its application. For a complete characterization of a solid No single technique is capable to characterize it, but it requires a number of characterization techniques to identify it (West, 2015).

Microscopic, Diffraction, and spectroscopic techniques are three main categories of characterization techniques which may be used to characterize non molecular and crystalline solids (Eral, 2006). Besides those Thermogravimetric analysis method has proven to be useful in characterizing solids (Ece, 2014). For a hybrid compounds with organic dyes thought to have luminescent properties, fluorescence spectroscopy can be utilized. (Skoog, 2007).

2.1. Microscopic Technique

The technique have been divided into two groups as optical and electron microscopes. The classical method of obtaining information was optical microscopy. However, scanning electron microscope (SEM) has proved to be bests for analysis of solids in order to get information about elemental compositions and morphology or surface topologies of the solids (West, 2015).

2.1.1. Optical Microscopy

Optical microscopy is used to examine particles down to a few micrometers under high magnification (Skoog, 2007). Optical microscopy is a cheap microscopic method that uses visible light to magnify objects and it has easy sample preparations. For selecting well defined crystals of the solid, the optical microscopy may be used to view the crystals under to pick them.

However, most conventional optical microscope uses visible radiation (wavelength 400–700 nm) and it cannot resolve images of samples that are smaller than half the wavelength of the light. Moreover, the diffraction effects limits the resolution of optical microscopy to that of the wavelength of light and only able to magnify samples only down to a few micrometer. Electron microscopy can magnify sub micrometer seized particles. For this reason they are more used than the optical microscopy (West, 2015).

2.1.2. Scanning Electron Microscope (SEM)

The Scanning Electron Microscope (SEM) is a microscope that gives information about the texture topography and surface features of powders or solid pieces by using electrons rather than light to form an image. Features up to tens of micrometers in size can be seen because of the depth of focus of SEM instruments. The resulting pictures have a definite 3-D quality. The resolution of SEM is approximately between 100Å and 10μm (West, 2015).

In analysis of the solid surface of the sample a high energy electron beam is scanned across. These incident electrons causes generation of lower energy secondary electrons and some manage to escape from the solid surface. These secondary electrons emitted from the sample are detected by getting attracted to the phosphor screen which glows. During this, photomultiplier measures the intensity of the light. In this way the topology and morphology of the sample is known (Skoog, 2007). Figure 2.1 gives how a secondary electron is generated from the surface of the sampled by the simple electron beam.

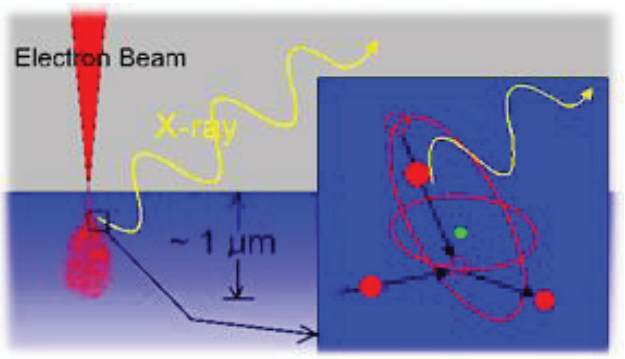

Figure 2.1. Electron beam scanning of surface (Source. Skoog 200)

SEM can also do the elemental analysis of the sample. This is done by focusing an electron gun to a small spot on the sample surface. SEM are most of the times equipped with the energy dispersive x-ray detector (EDX). This type of detector allows a user to analyze a sample molecular composition. The ideal specimen to be used for EDX microanalysis must be perfectly flat and polished. The results of EDX analysis are usually presented as a spectrum. The graphical representation of this spectrum has the *x*-axis representing the energy level which identifies the elements, and the *y*-axis gives the number of counts of each element detected (Eral, 2006)

The Philips XL-30S FEG Scanning Electron Microscope was used to analyze the obtained compounds. Samples were prepared for SEM analysis at room temperature.

2.2. Diffraction Techniques

The most common used diffraction methods are based on generation of X-rays by the X-ray tube. These X-rays are collimated and directed onto the sample, and diffracted rays from these are detected. For suitable diffracted ray is the angle between the incident and diffracted rays that must fulfill the Braggs condition of ($n\lambda=2d \sin\theta$). The wavelength of X-ray is related to the diffraction angle and the lattice spacing in a crystalline sample by this law. Powder and single crystal diffraction are the two good examples of these which only vary in instrumentation used (Skoog, 2007).

X-ray diffractometers consist of three basic elements: an X-ray tube, a sample holder, and an X-ray detector. X-rays are generated in a cathode ray tube by heating a filament to produce electrons, accelerating the electrons toward a target by applying a voltage, and bombarding the target material with electrons. When electrons have sufficient energy to dislodge inner shell electrons of the target material, electrons transition from outer shells occurs. These electrons take up the position left by the dislodged electron and characteristic X-ray spectra are produced (Joseph, 1999).

These spectra consist of several electron transitions. The most common being K_α and K_β which come from electronic transitions of shells (L to K) and (L to M) respectively (Skoog, 2007). The characteristic x-rays for each element can be generated by the electron beam knocking off the inner shell electron as shown in Figure 2.2. The x-ray are then captured by the detector and recorded.

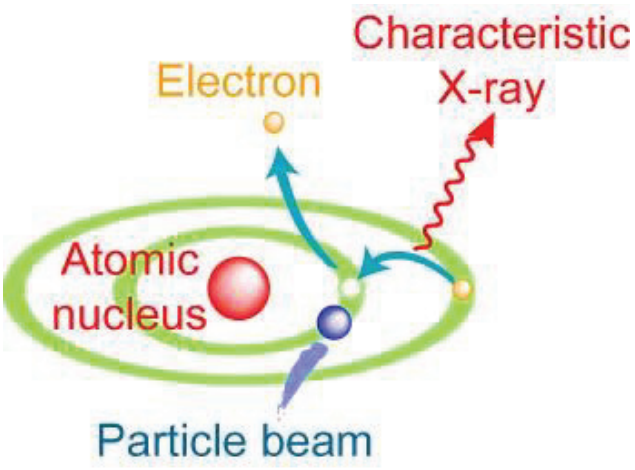

Figure 2.2. Generation of Characteristic X-rays (Source: Skoog, 2007).

The geometry of an X-ray diffractometer is such that the sample rotates in the path of the collimated X-ray beam at an angle θ while the X-ray detector is mounted on an arm to collect the diffracted X-rays and rotates at an angle of 2θ. The instrument used to maintain the angle and rotate the sample is termed a *goniometer.* As the sample and detector are rotated, the intensity of the reflected X-rays is recorded (Skoog, 2007). The Figure 2.3 shows how the diffraction of x-ray happens in the instrument.

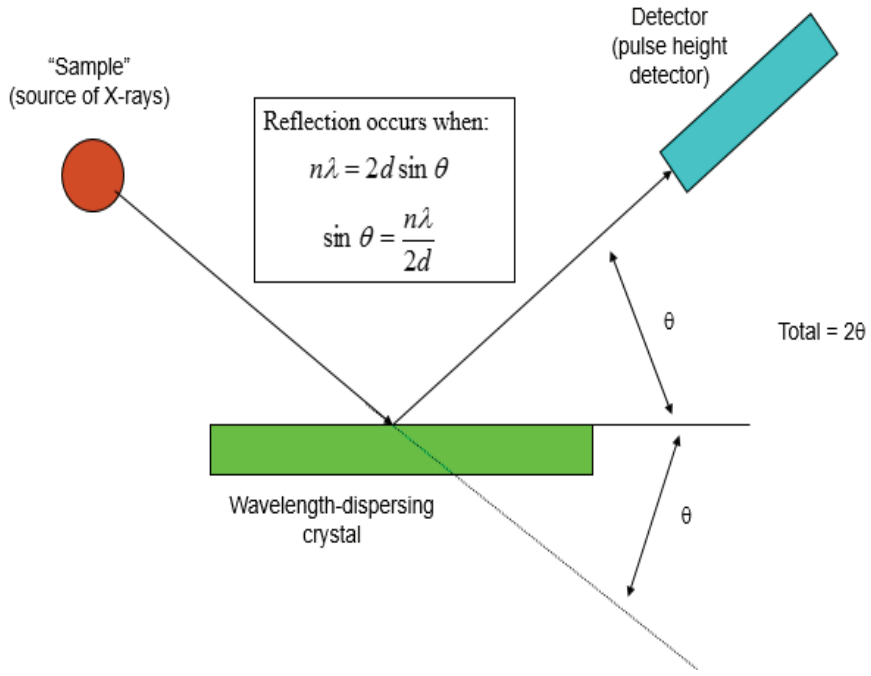

Figure 2.3. Diffraction of X rays (Source: Skoog, 2007).

When the geometry of the incident X-rays impinging the sample satisfies the Bragg Equation, constructive interference occurs and a peak in intensity occurs. A detector records and processes this X-ray signal and converts the signal to a count rate which is the n output to a device such as a printer or computer monitor. Results are commonly presented as peak positions at 2θ and X-ray counts (intensity) in the form of a table or an x-y plot. The relative intensity is recorded as the ratio of the peak intensity to that of the most intense peak.

2.2.1. X ray Powder Crystal Diffraction

X-ray powder diffraction (XRD) is a rapid analytical technique primarily used for phase identification of a crystalline material and can provide information on unit cell dimensions. The technique can be used to study the degree of crystallinity of a material, to determine the basic structure of the material, and to elucidate the degree of purity and crystallinity of the sample under interest. In this technique, fine randomly ground powder crystals are put in the path of monochromatic X ray beam, well angled oriented crystals diffracts these rays to fulfill the Braggs condition. These diffracted X-rays are then detected, processed and counted (Onen, 2011).

A flat film which is placed in front of the powder sample records a photograph consisting of concentric rings. This consist of a set of lines or peaks which have different intensities and position (d-spacing or Bragg angle) which are characteristic of a compound though intensity changes depending on sample preparations and the instrument used (West, 2015).

Joint committee for powder diffraction standards (JCPDS) contain an updated data library file of characteristic of thousands of crystalline substances. Every compound with the same crystal structure will produce an identical powder diffraction pattern, therefore the pattern serves as kind of a "fingerprint" for the substance, and thus comparing an unknown mineral to those in the Powder Diffraction file enables easy identification of the unknown. If X-ray powder pattern of the substance is not match with of the known phase, next step is collecting single crystal X-ray data (Ece, 2014). The synthesized compounds were analyzed by Philips X'Pert Pro Powder X-ray Diffractometer with Cu Kα radiation at 40 keV and 30 mA, and scanning rate was set to 3 min^{-1} in the 2h range.

2.3. Spectroscopic Techniques

There are a lot of different spectroscopic techniques. Actually all of them are based on the same principle. Under certain conditions materials can absorb or emit electromagnetic radiation which can take different forms. These techniques have a spectra which consist of a plot of intensity of absorption or emission (y axis) as a function of energy (x axis). The energy axis is usually expressed with frequency or wavelength (Skoog, 2007).

2.3.1. Fourier-Transform Infrared Spectroscopy (FT-IR)

Infrared absorption spectroscopy is a very powerful tool for determining the identity and structure of both inorganic and organic compounds. An IR spectrum is the plot of intensity of absorption as a function of frequency or wavenumber. It is possible to obtain an IR spectrum from samples in many different forms, such as liquid, solid, and gas. IR spectroscopy has been used as a qualitative tool to provide mostly information about the presence or absence of certain functional groups for organic compounds by using reference spectra (Skoog, 2007).

The method involves triggering molecular vibrations by irradiation of the material with infrared light. Vibrational modes, which include pairs or groups of bonded atoms, may be excited to higher energy states by absorption of radiation of appropriate frequencies. Some of frequency of the incident radiation are not absorbed but passes through the sample of compound or transmitted by the sample The detector measures the transmitted frequencies, and by doing so also reveals the values of the absorbed frequencies (West, 1991).

Fourier transform infrared (FTIR) spectrometers are the preferred choice for samples that are energy-limited or when increased sensitivity, resolution, and speed of data acquisition is desired. The FT-IR spectrometer has an Interferometer which has makes it have better performance than ordinary IR machine (Skoog, 2007). For this reason the FT-IR is preferred over ordinary IR machine in carrying out analysis of samples. FT-IR spectroscopy gives characteristic region of Inorganic solids spectrum between 1000-400cm^{-1} due to metal-oxygen stretching vibrations. Other than that the

obtained data can be used for identification of unknowns such as covalently bonded hydroxyl groups, trapped water, carbonate, nitrate etc (West, 1991).

The FT-IR was recorded with a Perkin Elmer Spectrum 100 FT-IR spectrometer using KBr pellets between 4000 and 400 cm^{-1} range. In this method, 2.5 mg sample was mixed with 250 mg KBr. Then, this mixture was ground by using mortar and pestle and placed inside a die. It was held under hydraulic press of 10000-psi pressure varied at 5 minutes in order to form a pellet. After that, the mixed pellet was placed inside the spectrometer port for the measurement run in transmittance mode.

2.3.2. Proton Nuclear Magnetic Resonance Spectroscopy (^{1}H NMR)

This is a research technique that exploits the magnetic properties of the protons (^{1}H) nuclei. The intramolecular magnetic field around a protons in a molecule changes the resonance frequency, thus giving access to details of the electronic structure of a molecule. Most frequently, NMR spectroscopy is used by chemists to investigate the properties of organic molecules, although it is applicable to any kind of sample that contains nuclei possessing spin (Solomon, 2013).

The continuous wave (CW) method is simplest procedure for obtaining the spectrum. A typical CW-spectrometer is shown in the diagram in Figure 2.4. A solution of the sample into an NMR glass tube is oriented between the poles of a powerful magnet. Radio frequency radiation (rf) of appropriate energy is broadcast into the sample from an antenna coil. A receiver coil that surrounds the sample tube, detects and emission of absorbed rf energy which is monitored by dedicated electronic devices and spectrum processed by a computer (Skoog, 2007).

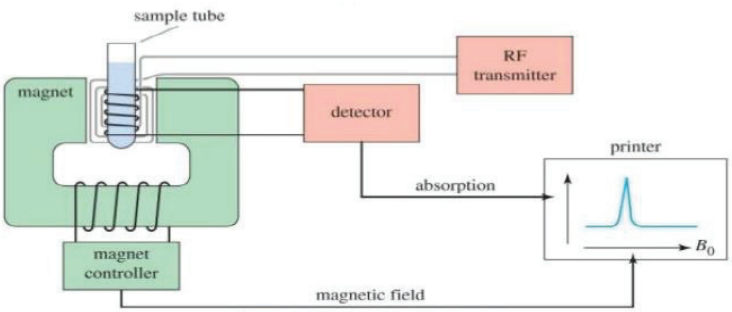

Figure 2.4**.** The continuous wave spectrometer (Source: Skoog, 2007).

There are two ways in which this NMR spectrum is acquired. One depends on varying or sweeping the magnetic field over a small range while observing the rf signal from the sample. The other varies the frequency of the rf radiation while the external magnetic field is kept constant (Keala, 2009).

In ^{1}HNMR spectroscopy, chemically equivalent protons gives rise to the number of signals in the spectrum. Chemically Equivalent Protons are identical protons that are in the same chemical environment. Therefore, these protons will only show one peak signal in the spectrum.

The positions of the proton signals in based on how far they are from the signal of the reference compound. Normally, this data signal observed gives the chemical environment of the proton or protons that are responsible for the signal. Tetramethylsilane (TMS) is the preferred reference compound used in ^{1}HNMR analysis. The main reason for the use of this compound is that all the methylene protons are chemically equivalent. Furthermore the volatility of TMS makes e easy removal from the sample by evaporation.

The chemical shift determines the position of the proton signals. Chemical Shift is defined as a measure in parts per million (ppm) of how far the signal produced from the proton is from the reference compound signal. Usually in NMR analysis. The chemical shift is measured by use of the delta scale. Protons that are closer to the electronegative atom are in a less electron dense environment, which means that their chemical shifts will be larger. The terms *upfield* or *downfield* is used to designate the proton position if it is further to the right hand side or further left side of the spectrum respectively.

The area under each peak signal is proportional to the amount of radio energy and number of equivalent protons that give rise to that signal. Integration of this area measurement will therefore give the relative number of protons that are responsible for such signal.

Splitting of signals is caused by protons bonded to adjacent carbons. Using (N+1) Rule where N is the number of equivalent protons gives the multiplicity of the non-equivalent proton signals that are bonded to the adjacent carbons. Spin-spin coupling occurs between non-equivalent neighboring protons that's leads to splitting. Coupling Constant (J) is how far is the two adjacent peaks of a split signal of the protons. The

effect of each of the coupled proton nuclear spins determines magnitude of this coupling constant (Solomon, 2013).

2.3.3. Fluorescence Emission

This is a type photoluminescence process in which atoms or molecules are excited by absorption of electromagnetic radiation then photons are emitted from electronically excited states. Luminescence is the term exclusively used for all light emissions, but fluorescence only denotes light emissions of allowed transitions from higher to lower excited singlet states of molecules which only last in nanoseconds range (Joseph, 1999). When sample molecules are exposed to light having an energy that matches a possible electronic transition within the molecule, some of the light energy will be absorbed as the electron is promoted to a higher energy orbital. The electron then after begin to relax, as it does so it emits photon (Skoog, 2007).

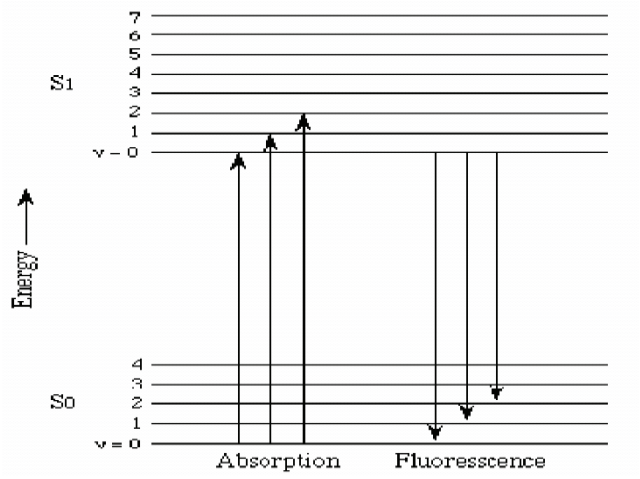

Figure 2.5. Fluorescence spectroscopy (Source: Skoog, 2007).

As shown in Figure 2.5, energetically favored electron promotion will be from the highest occupied molecular orbital (HOMO), usually the singlet ground state, S_0, to the lowest unoccupied molecular orbital (LUMO), and the resulting species is called the singlet excited state S_1. The energy of the emitted photon is lower than that of the incident photons of absorption. Electron return from excited singlet state to ground state; does not require change in spin orientation which is the more common form of relaxation.

The efficiency of the fluorescence process is measured by the quantum yield. By definition, the fluorescence quantum yield Φ_F expresses the portion of excited molecules that deactivate by emitting a fluorescent photon. It is the ratio of the number of emitted photons to the number of absorbed photons per time unit (Joseph, 1999).

Not all compounds can show fluorescence unless it's a fluorophore. A fluorophore absorbs energy of a specific wavelength and then later emit energy at a different but equally specific wavelength. The chemical environment of the fluorophore determines the amount the emitted energy. Fluorophores are also referred to as chromophores, which is the part or moiety that gives the color of a molecule. However, this chromophore denotation implies that the molecule absorbs energy while fluorophore means that the molecule can also emit energy (Skoog, 2007). Usually most fluorophores have high absorption in the visible part of the spectrum. Most of the structures that are fluorophore are:

- Aromatic or a compound that possess several conjugated double bonds
- Rigid molecule and complexation leads to no bond rotation

Quenching is the term used to refer to the decrease in fluorescence maximum wavelength of emission. This is caused by non-radiation emissions which lead to lowers the wavelength. Some compounds attached to the fluorophore can make it either to reduce or totally to lose all its fluorescence (Joseph, 1999).

2.4. Thermogravimetric Analysis

Thermogravimetry (TG), the technique in which the mass of a sample is monitored against time or temperature, is performed with a Thermogravimetric Analyser (TGA) or thermobalance. The sample on the scale is heated over wide range of temperature and the change in weight is monitored. A plot of mass as a function of time or temperature is the result of a thermogravimetric experiment (Groenewald, 2001).

Thermogravimetric studies provide data on changes in mass as a function of time or temperature. Continuous mass recording and compensation is possible by electromagnetic weight compensation. Sensitivities are usually several micrograms. Total sample masses may range from milligrams to grams. Temperature ranges are usually from room temperature to as high as 2700K.

The results are given as a continuous chart record. In this method, a few milligrams of sample is weighed and heated at a constant rate in the range from 1 to 20˚C min^{-1}. Sample has a constant weight until it starts to decompose at initial temperature. Decomposition generally occurs over a range of temperatures, initial temperature to final temperature and a second constant weight plateau is observed above the final temperature that corresponds to the final weight of the sample. Initial weight, final weight and the difference between them are the basic properties of the sample and they are used for quantitative calculations of compositional changes. On the other hand, initial and final temperatures are based on heating rate, the nature of the solid and the atmosphere above the sample (West, 2015).

Major applications of thermogravimetry involve thermal stability analysis of materials in different atmospheres or vacuum and purity determination of the sample. In addition it use to determine the amount of crystal water present in the sample. The Perkin Elmer Diamond TG/ DTA instrument was used to analyze our samples. The nitrogen gas atmosphere was used with heating at a specific temperature rage for each sample.

CHAPTER 3

EXPERIMENTAL

3.1. Reaction Autoclaves

These are vessels used for hydrothermal reactions. The reactants are put into the vessel placed into the oven set at the certain temperature under specified time. There are some important qualities which an ideal autoclave must possess like inertness to any reactants in it, to work at high pressures and temperatures and to be leak proof (Byrappa, 2001).

In addition to that, Autoclaves are sold by a number of vendors, inexpensive, easy to handle, and require no special auxiliary equipment. The main disadvantage of these autoclaves is that the fluoro polymer liner will begin to deform and weaken with temperatures exceeding 240^{o}C. Thus, the autoclave cannot contain fluids approaching true supercritical aqueous fluids. (Eral, 2006).

Therefore, they have become the primary vessel for hydrothermal work done below 200^{o}C. Usually a Polytetrafluoroethylene (PTFE) line acid digestion bomb are used as reaction autoclave with a Teflon lining. The Teflon having a suitable coefficient of thermal expansion makes it possible to maintain the pressure when the material enclosed in it expand with a spring loaded closure. Teflon will expand and contract much more upon heating and cooling cycles than its enclosure material (Byrappa, 2001). Below (Figure 3.1) shows the components of the autoclave used to prepare POM-organic hybrid.

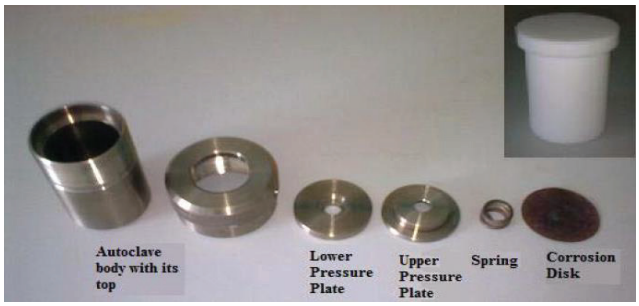

Figure 3.1. Steel autoclave and Teflon vessel. (Source: Onen, 2011).

The general procedure for Hydrothermal Synthesis of an inorganic-organic hybrid is that, the POM and an Organic ligand which are the starting materials are put in the autoclave. This is then filled with water and mineralizer which enhances the solubility of the reactants. The required pressure with water fill and the optimum pH are maintained for the reaction to occur by dissolution and precipitation. The reaction mixture is then put in the oven (Figure 3.2) set at the desired temperature and time of heating. The autoclave is cooled slowly at room temperature and after, the product is isolated by filtration and washed to obtain pure crystal. The product then can be identified by using some characterization techniques (Ece, 2012).

Figure 3.2. Steel autoclave placed in oven. (Source: Onen, 2011).

3.2. Materials

All the laboratory chemicals used were reagent grade, purchased from commercial sources and used without further purification. Some compounds were synthesized according to procedures described in literature with minor changes.

3.3. Preparation of Keggin-Amide Hybrids

Literature methods were followed wıth minor changes to prepare precursors. The amıdation reactıon was carrıed out by reacting the grafted organotın wıth carboxylic acıd group and four organic amine. This was done by using dicyclohexyl carbodiimide (DCC) which acted as a coupling agent. The reaction mixture was refluxed for two days and passed through rotary evaporator. The amide product obtained was characterized by FT-IR, TGA and PXRD.

3.3.1. Synthesis of Mono-Lacunary Keggin $K_7[PW_{11}O_{39}].14H_2O$

68mg of Na_2HPO_4 (358.00 g/mol) was put a beaker containing 10 mL water. 660mg of $Na_2WO_4.2H_2O$ (329.55 g/mol) was added to this. The reaction mixture was then to t 70~80 ℃ with stirring for and PH kept at 3.0 with addition of 1M H_3PO_4. 284mg of KCl (74.55 g/mol) was then added and left overnight. The white precipitate formed was filtered under vacuum, and washed with cold water to get the final white solid (480mg, 92% yield).

$$Na_2HPO_4 + Na_2WO_4.2H_2O + H_2O + KCl \rightarrow K_7[PW_{11}O_{39}].14H_2O \quad (3.1)$$

3.3.2. Synthesis and Characterization of $Cl_3SnCH_2CH_2COOH$

The method published on synthesis of $Cl_3SnCH_2CH_2COOH$ denoted as **Sn-COOH** was followed with minor slight changes. (Shan 2014) Anhydrous $SnCl_2$ (0.1g, 190.48g/mol) and acrylic acid CH_2=CHCOOH (0.1mL, 72.00g/mol) was added to a flask containing diethyl ether at RT.

Anhydrous HCl gas was then slowly passed through this mixture delivered from the reaction of NaCl and H_2SO_4. The excess HCl gas was left to escape. The final amorphous white powder obtained was vacuum dried and corresponded spectroscopically to Sn-COOH (yield: 1.2g, 90%).

$$CH_2=CHCOOH \xrightarrow[Et_2O.\ RT]{HCl,\ SnCl_2} Cl_3SnCH_2CH_2COOH \quad (3.2)$$

3.3.3. Synthesis of $TBA_4[PW_{11}O_{39}SnCH_2CH_2COOH]$

To the lacunary Keggin POM $K_7[PW_{11}O_{39}]14H_2O$ (0.28g, 3202.87 g/mol) dissolved in 30 mL of water, $Cl_3SnCH_2CH_2COOH$ (0.002g, 298.21 g/mol) was added. The PH of the resulting reaction mixture was maintained at 3.1 by dropwise adding 1 mol/L KOH. After stirring for 15 minutes at room temperature, the mixture was filtered and the obtained solution was precipitated by addition of tetrabutylammonium bromide (TBBr) (0.10 g, 322 g/mol).

The mixture was stirred for 1 h at room temperature and then solid was filtered off. Evaporation of **the** solvent resulted in a pale yellow oily solid which was confirmed spectroscopically as a final product denoted as **TBA-K_{Sn} [COOH]** (Yield: 0.27g. 87%).

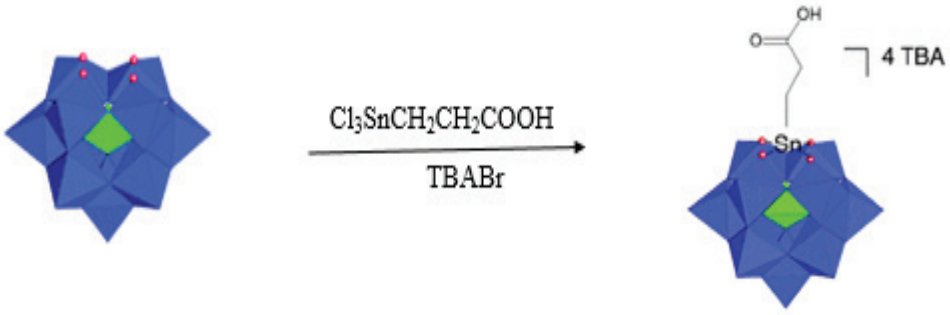

(3.3)

3.3.4. Synthesis of $TBA_4[PW_{11}O_{39}SnCH_2CH_2CONHR]$

TBA-K_{Sn} [COOH] (1.3 mmol; 1 equiv; 585 mg) was added to a solution of DCC (0.20 mmol; 1.5 equiv; 37 mg) dissolved in acetonitrile 10 mL CH_3CN in round-bottomed flask equipped with a condenser and a magnetic stirrer. After 15 min of stirring, the amine R-NH_2 (0.4mmol, 1 equiv) was then added to the solution. As shown in table 3.1 three different organoamine in ethylendiamine, Leucine and 3-Aminophenol were reacted. The reaction mixture was then kept overnight under reflux.

10ml of acetone was added and the resulting mixture stirred for 1hour under rotary. The solid was filtered off and concentration of the solvent under vacuum afforded a pale yellow oil like solution which was precipitated (ethanol/Et_2O. 1:10) to give the desired final white solid amide product denoted as **TBA-K_{Sn} [CONHR].**

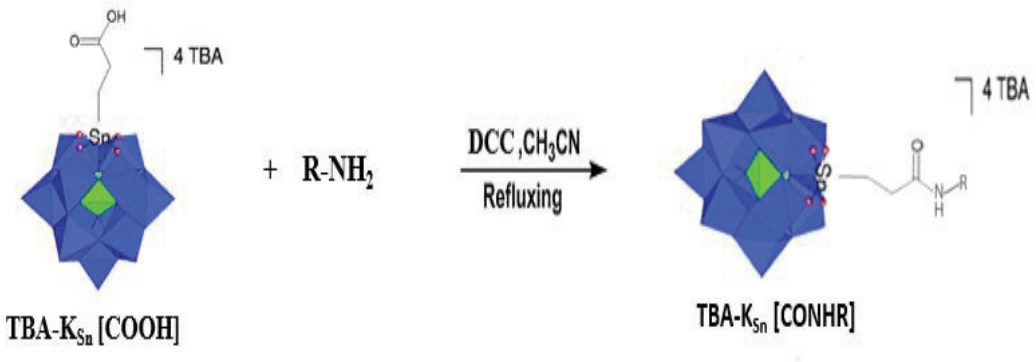

(3.4)

Table 3.1: Organic moiety used with amine group

Entry	Nucleophile (R-NH_2)	Mass (g)	Yield (%)
1	**Ethylene diamine**	**-**	**-**
	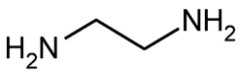		
2	**Leucine**	**0.458**	**89**
	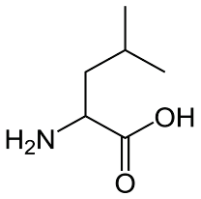		
3	**3-aminophenol**	**0.385**	**71**
	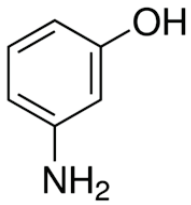		

3.4. Synthesis of Lindqvist POM-BODIPY Hybrid

The Lindqvist POM was prepared by following the literature procedure. Thıs was then reacted with the phosphıne based BODIPY derivative. The BODIPY derivatıve was synthesized by from the organic lab and obtained as a brown-reddısh powder. The synthetic pathway chosen was shorter than the on prescribed ın literature. The temperature and pH of the reaction were maintained. The final product was characterized by FT-IR, SEM, PXRD and TGA.

3.4.1. Synthesis of Lindqvist POM ($Na_2W_6O_{19}$)

$Na_2WO_4 \cdot 2H_2O$ (60mg, 2.45 mmol) was added to 0.5 mL DMF at the temperature 40 °C. The solution was stirred for 10 min and 0.1 mL acetic anhydride was added slowly. This was again stirred for another 5 min and 0.1 mL HNO_3 was very slowly added. A bright yellow solution formed which was left stay overnight. The precipitate formed was then filtered under vacuum and washed with diethyl ether. This was repeated 2 times to get of a white solid (45mg, 89.5%).

$$Na_2WO_4.2H_2O + HNO_3 \xrightarrow[DMF,\ 40\ °C]{\text{Acetic Anhydride}} Na_2W_6O_{19} \qquad (3.5)$$

3.4.2. Hydrothermal Synthesis of Lindqvist POM-BODIPY Hybrid

25mg (2.0mmol) of the Lindqvist POM $Na_2W_6O_{19}$ was added to 10mg (2.0 mmol) of the BODIPY dye dissolved in 0.3 mL DMF. The reaction mixture was the stirred with heating at the temperature of 40 °C for 3hrs. This was then dried with a rotatory evaporator forming a yellow solid immediately. This solid was collected and washed 3 times with methanol and ethyl ether to obtain a brown solid (yield: 28mg, 91.21%).

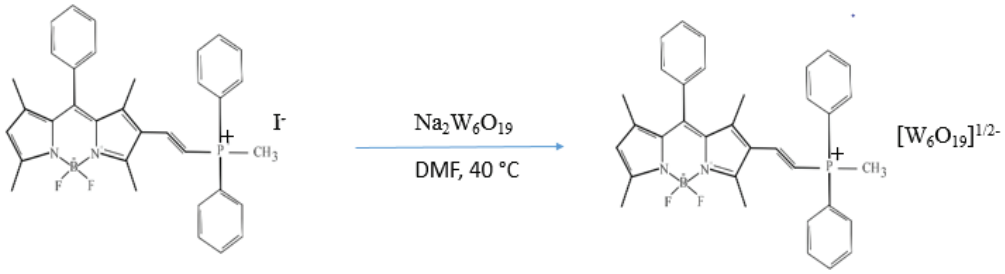

(3.6)

CHAPTER 4

RESULTS AND DISCUSSION

The association of the POM and organic compounds has been known to form hybrids with improved properties. Some of such properties is the altering the fluorescence properties in the hybrid material formed (Matt, 2011). It is from this background that it was thought to develop a hybrid based on the rarely combined forms of POM and BODIPY derivative dyes.

Therefore, an organo-tin grafted monolacunary Keggin POM grafted with side chain having carboxylic acid was successfully combined with an organic derivative with an amine group (Table 3.1). Unfortunately efforts to form the hybrid with a BODIPY derivative this reaction was unattained. This was due to its unavailability and the long procedure required to prepare the BODIPY amine containing derivative which could not carter with the time of this report writing.

However, two amine containing organic compounds of Leucine and 3-aminophenol were successfully used to undergo the amidation reaction with the carboxylic acid functionalized Keggin POM. Despite the many step reactions involved in the synthesis of the final product, the Keggin structure showed stability by not decomposing and remained intact. The coupling agent of this amidation reactions chosen was DCC due to its availability in the organic lab and easy removal after the reaction.

Furthermore, based on works of Jin Bakaong (2010) in shown in Figure 1.8 the Lindqvist POM can self-assemble with an organic dye to give a very thermally stable hybrid. This idea was used successfully used in the synthesis of novel organic-inorganic hybrid material of Lindqvist POM and BODIPY dye by hydrothermal method. The hybrid material formed showed loss of fluorescence with respect to the phosphine based BODIPY derivative as no peaks were observed during the analysis. This clearly showed that the fluorescence properties of the dye were altered.

The final products in all the successful synthesis were characterized by FT-IR and TGA. SEM/EDX and powder XRD were also employed to characterize precursor compounds.

4.1. Keggin-Amine Hybrids

Tungsten based POMs are so robust that they have been used to develop many inorganic-organic hybrids. Keggin polyanion structure has attracted much interest by many researchers due to the relatively easy formation of lacunary anions. In this regard, an organic tungsten Keggin POM-based $TBA_4[PW_{11}O_{39}SnCH_2CH_2COOH]$ precursor was synthesized by following a previously reported procedure (Shan: 2014). The amidation reactions between the carboxyl group and number of amine containing species have been extensively studied.

The mono-lacunary Keggin POM of $K_7[PW_{11}O_{39}].14H_2O$ was obtained as a white precipitate of the product and characterized (equation 3.1). The FTIR spectrum (Figure 4.1) obtained was compared with the one reported in literature which showed the most similar major peaks meaning the mono-lacunary Keggin was successfully synthesized. The product gave the IR spectrum with major vibrations a broad band of 3421.60cm^{-1} for $\nu(H_2O)$. The oxygens bonded to the heteroatom Phosphorus $\nu(P-O_a)$ gave two vibrations 1080.33$cm^{-1}$and 983.07cm^{-1} , the terminal bonded oxygen $\nu(W-O_d)$ had 890.74cm^{-1}. The three bridging oxygen gave vibrations $\nu(W-O_c-W)$ for 811.14cm^{-1} , $\nu(W-O_b-W)$ was 595.33cm^{-1} and $\nu(W-O_a-W)$ was 526.25cm^{-1}. Therefore, we have concluded that the mono-lacunary Keggin $K_7[PW_{11}O_{39}].14H_2O$ was successfully synthesized.

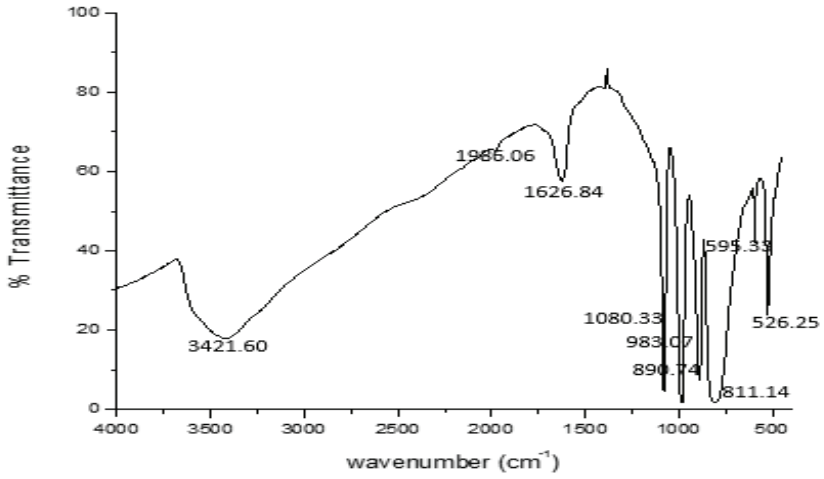

Figure 4.1. FT-IR spectrum of $K_7[PW_{11}O_{39}].14H_2O$

The morphology of the compound obtained with the SEM image. The SEM showed the clear Morphology of the crystals formed (Figure 4.2)

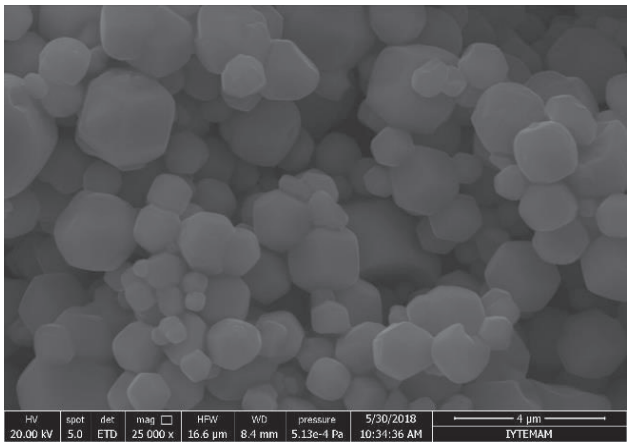

Figure 4.2. SEM images of $K_7[PW_{11}O_{39}].14H_2O$

The SEM/EDX spectrum of the $K_7[PW_{11}O_{39}].14H_2O$ crystal are shown in Figure 4.3. In accordance with the results, the synthesized compound contains tungsten, sodium, oxygen and phosphorus elements in the weight percentages shown.

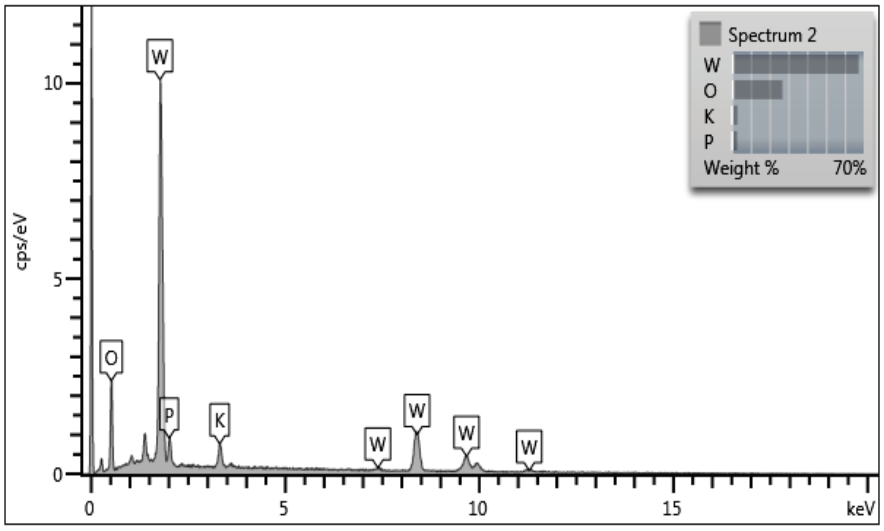

Figure 4.3. SEM/EDX spectrum of $K_7[PW_{11}O_{39}].14H_2O$

In Table *4*4.1, the results showed the presence of elements by percent weight of K – 2.97, P – 2.81, W – 67.43 and H_2O – 26.88%. The Analytically calculated value has

For $K_7[PW_{11}O_{39}]\cdot 14H_2O$: K - 8.54, P - 0.97, W - 63.14, H_2O - 7.86 %. Therefore, the EDX results shows similarity and henceforth the compound was successfully synthesized.

Table 4.1**:** The EDX results of $K_7[W_{11}O_{19}].14H_2O$

Element	**Weight (%)**	**Atomic (%)**
O	26.88	75.92
P	2.81	4.10
K	2.97	3.43
W	67.34	16.55
Total:	100.00	100.00

The powder X-ray diffraction pattern of the title compound $K_7[PW_{11}O_{39}].14H_2O$, was obtained as shown in Figure 4.4. The Powder XRD results is in good agreement with the literature and it showed a clear baseline indicating the pure product was obtained.

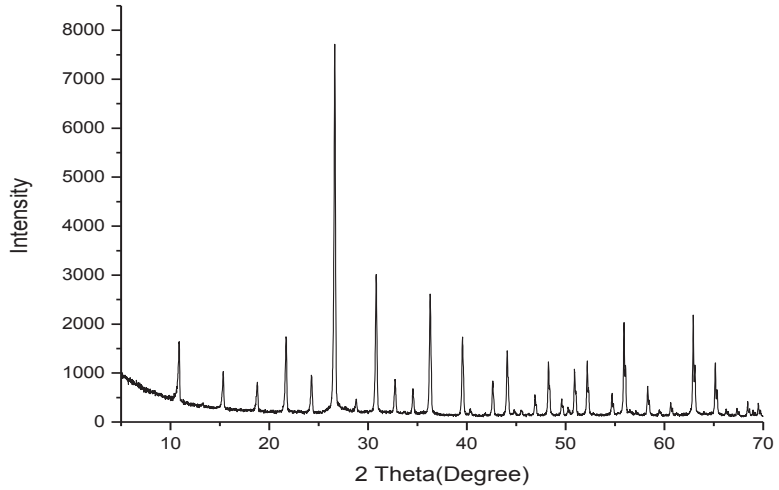

Figure 4.4. Powder XRD spectrum of $K_7[PW_{11}O_{39}].14H_2O$

In the following step as shown in equation 3.2, the compound $Cl_3SnCH_2CH_2COOH$ was synthesized from anhydrous tin(ii) chloride with slightly excess of anhydrous HCl and acrylic acid in ether. The white solid powder obtained corresponded analytically and spectroscopically with the one in literature. The FT-IR spectrum shown in Figure 4.5 a broad vibration for carboxylic acid ν(0-H) at 3311.56cm^{-1}. The appearance of two Sharp vibrations at ν(C−H)= 2981.84cm^{-1} and ν(C−H)= 2821.71cm^{-1} corresponding to the alkene protons. The relatively low frequency carbonyl stretching ν(C−O) was observed at 1636.74cm^{-1} . A sharp strong stretching vibration at 1487.31cm^{-1} was deduced to be coming from the ν(Sn−C).

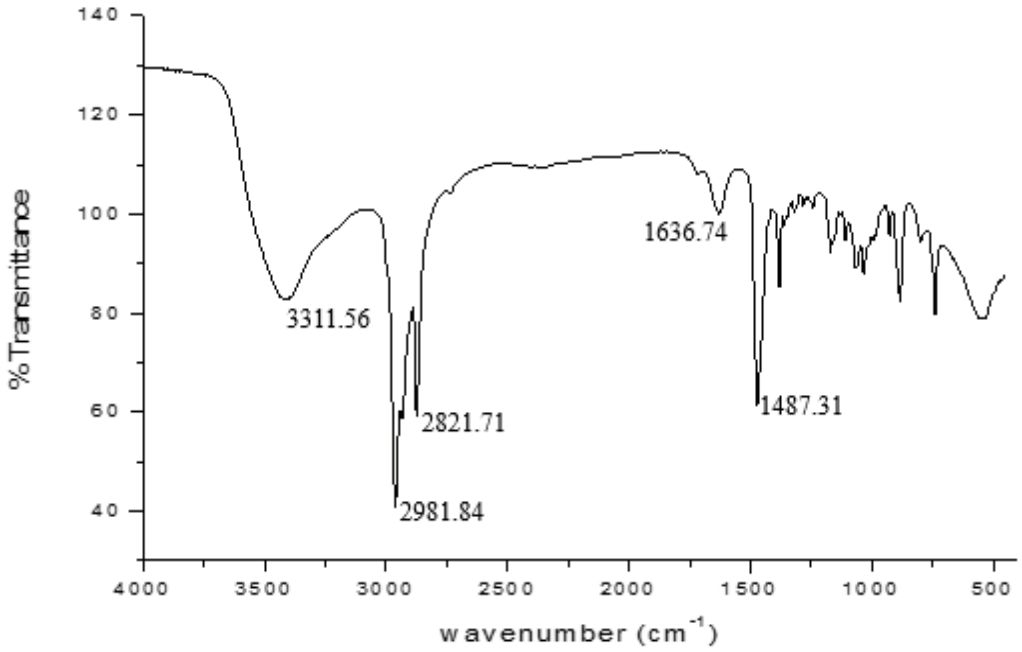

Figure 4.5. FT-IR spectrum of Sn [COOH]

The monovacant lacunary Keggin $[PW_{11}O_{39}]^{7-}$ in water was then successfully grafted with an organic part $Cl_3SnCH_2CH_2COOH$ through the formation of Sn-O bonds (equation 3.3). During the reaction, the pH at 3.1 was maintained by addition of aliquots of a 1 M KOH solution to avoid the competitive formation of the complete Keggin structure $[PW_{12}O_{40}]^{3-}$ (Matt: 2012). After filtration of the solution, addition of tetrabutyl ammonium bromide led to the precipitation of the POM as a tetrabutyl ammonium (TBA) salt **$TBA_4[PW_{11}O_{39}]Sn(CH_2)_2COOH$** denoted as TBA-$K_{Sn}$[COOH].

The spectra obtained for each analysis exhibits signals from both the Organic part, TBA cation as well as the Keggin cluster. A detailed analysis shows an IR display (Figure 4.6) of a characteristic pattern of the Organotin grafted Keggin type POM with major stretching vibrations. The broad peak at 3421.60cm^{-1} which was attributed by the carboxylic ν(0-H). The appearance of a strong Sharp peak at 2991.82cm^{-1} and medium 2821.71cm^{-1} was from the alkane ^{1}H which could come from the grafted side chain and from TBA. A low frequency stretching peak at 1637.88cm^{-1} was coming from the ν(C−O). A strong stretching from the Keggin for ν(P−O_a) was obtained at 947.17cm^{-1} showing that it was part of the compound. It can be deduced from the spectrum that, in the low wavenumber region (<1100 cm^{-1}), the disappearance of the ν(P-O_a)asymmetric vibration at 1080.33 cm^{-1} showed the vacant site of lacunary [$PW_{11}O_{39}$] clusters was filled with formation of Sn-O bonds. Furthermore, the bands in the 1500–3500 cm^{-1} region are due to characteristic vibration of the organic moieties. This results indicate that high yield of 81.2% for TBA-K_{Sn}[COOH] was obtained in the solid state with retention of Keggin structure and had interactions with organic moieties.

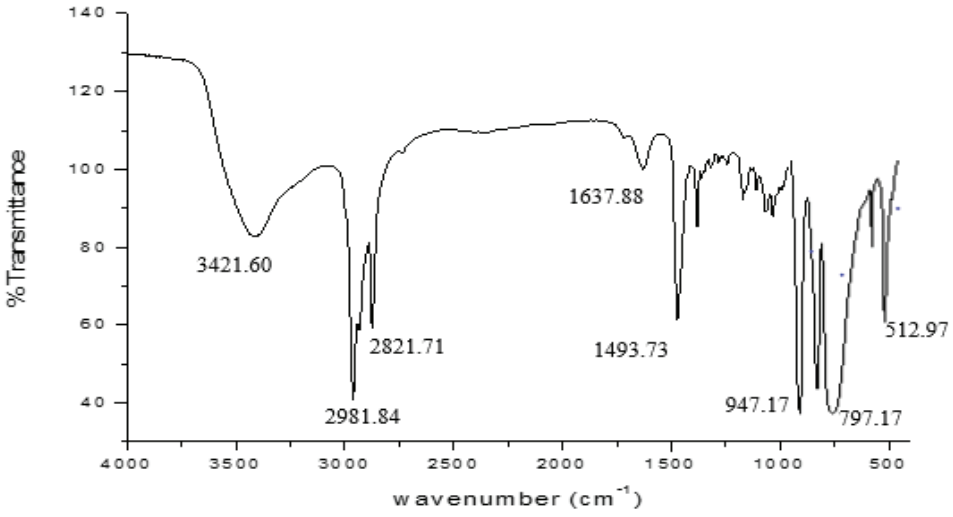

Figure 4.6. The IR spectrum of TBA-K_{Sn}[COOH]

In the synthesis of TBA-K_{Sn} [CONHR] as shown in equation 3.4, the appearance of the amide signals gave strong evidence that the organic moieties with the amine group were successfully coupled to the organic arm of the Keggin POM. All the synthesis were done in 2 days of refluxing with DCC used as a coupling agent and acetonitrile as solvent.

It was necessary to add an excess of the organic amine to get total conversion of the POM. The byproduct removed by washing two times with the ethanol/ether mixture to give the desired amide product. The amidation reaction with ethylene diamine did not give the expected product. Perhaps the 2 days given was short, therefore lead to unsuccessful completion of the reaction.

The amidation reaction with 3-aminophenol gave the product **TBA [K_{Sn}CO-Ph]** in good yield (71%).

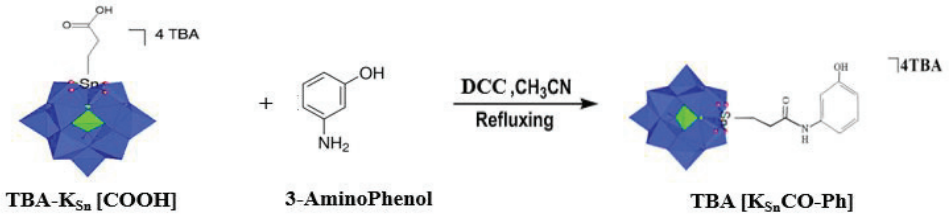

The FT-IR spectrum (Figure 4.7) of a compound formed from 3-aminophenol TBA [K_{Sn}CO-Ph] exhibits an amide *ν*(N-H) with characteristic stretching band at 3623.41cm^{-1}. It also shows the Phenol *ν*(O-H) at 3320.23cm^{-1}, the methylene *ν*(C-H) at 2978.12cm^{-1} and carbonyl amide ν(C=O) Stretch at 1670.87cm^{-1}. A medium peak absorption Aromatic C-H Stretch at 3027cm^{-1}. The stretching vibrations from these peaks can be strongly believed that the amidation reaction with 3-Aminophenol was successful.

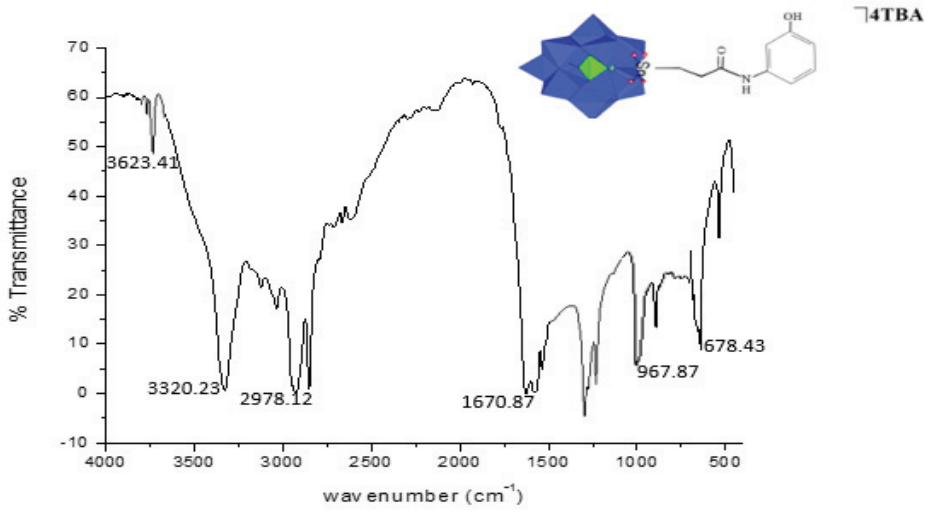

Figure 4.7**.** The FT-IR of TBA [K_{Sn}CO-Ph]

The thermogravimetric analysis of the TBA [K_{Sn}CO-Ph] were determined under a nitrogen atmosphere with a heating rate of 10 °C·min^{-1} in the temperature range from room temperature to 1000 °C. In the Figure 4.8, the TGA curve of the compound exhibits great stability until it reaches 300 °C when there is a sudden weight loss. This first weight loss of 35.67% was between 300 and 350 °C, which was due to the loss of the organotin and 3-Aminophenol group. The second weight loss of 38.17% in the range of 350–510 °C can be ascribed to the complete decomposition of the tetrabutylammonium cation (TBA^+) and the residue of the POM cluster $[PW_{11}O_{39}]^{7-}$. Consequently, all the organic moieties of the hybrid might have been also completely decomposed at 510 °C.

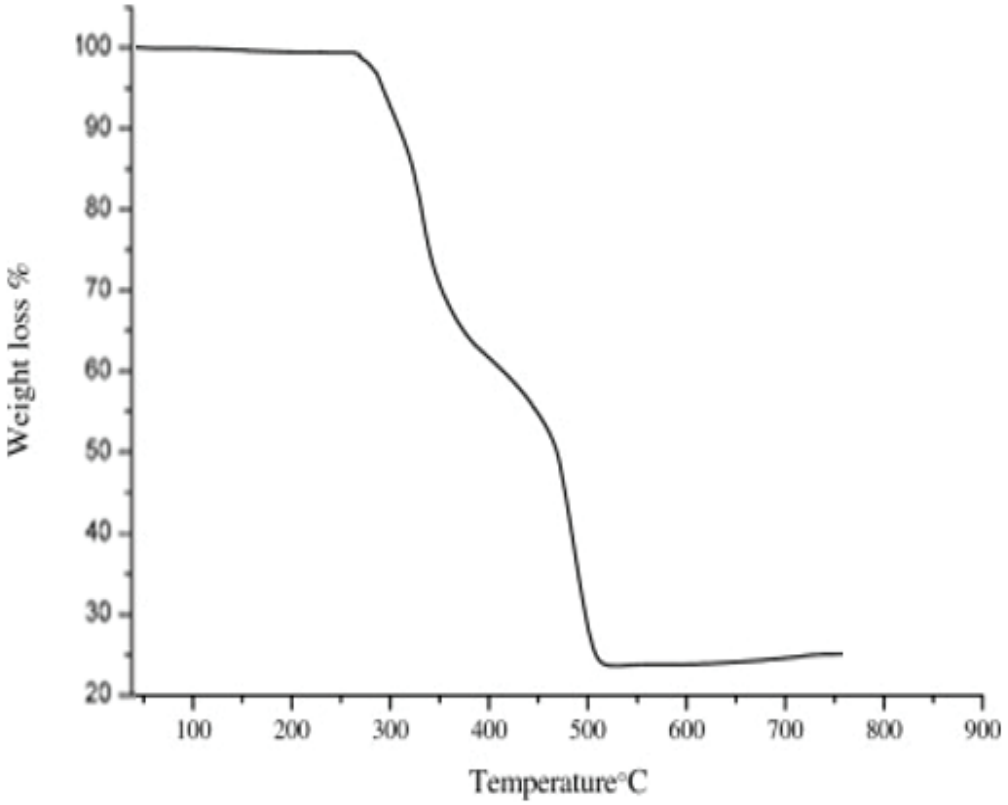

Figure 4.8. The TGA curve of TBA [K_{Sn}CO-Ph]

The Table4.2 shows the weight losses obtained with the calculated theoretical weight loss of the compound. It can be observed that the obtained weight losses of the compound are in agreement with the theoretically calculated values. These results are in conformity and perfectly confirms the compound TBA [K_{Sn}CO-Ph] was obtained.

Table 4.2. The TGA weight losses with temperature of TBA [K_{Sn}CO-Ph]

Residue	**Temperature (°C)**	**Actual Weight loss (%)**	**Theoretical Weight Loss (%)**
Organotin/3-Aminophenol	300 – 350	35.67	36.23
$TBA^{4+}/[PW_{11}O_{39}]^{7-}$	350 – 510	38.17	40.89
WO_3	> 510		

The Powder XRD experiment was carried out on TBA [K_{Sn}CO-Ph] compound in order to observe its crystalline phase purity. The obtained patterns (Figure 4.9) of the samples was consistent as it indicated the presence of one crystalline phase which corresponded to the compound.

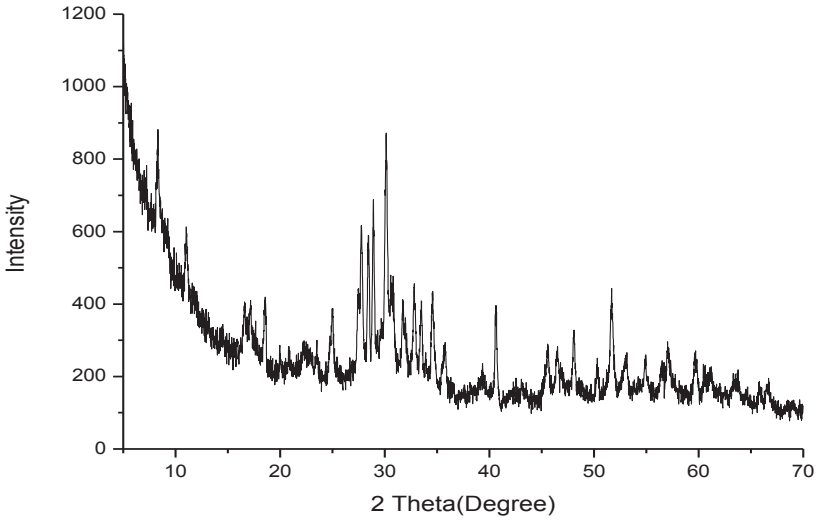

Figure 4.9. The obtained Powder XRD of TBA [K_{Sn}CO-Ph]

The functionalized organotin Keggin also reacted with Leucine to give the product **TBA [K_{Sn}CO-Leu]** in good yield (89%).

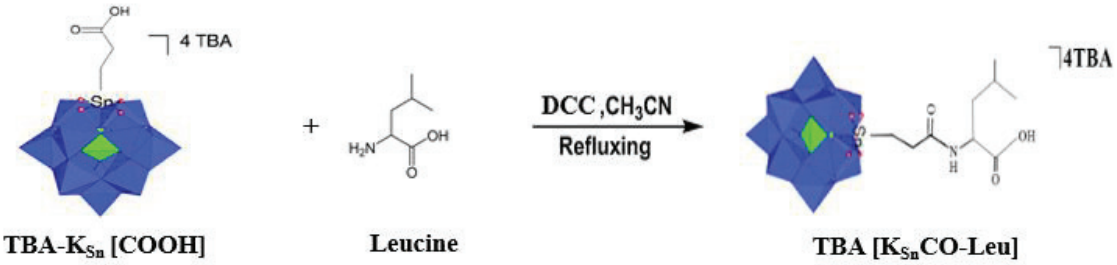

The FT-IR spectrum (Figure 4.10) of TBA [K_{Sn}CO-Leu] shows the characteristic signal that confirms amide formation. The signals at 3597.05cm can be attributed to the amide *v*(N-H) in comparison with the spectra of the precursor which had no such a signal. While after amide coupling the signal for the methylene protons at group 2932.12cm^{-1} were overshadowed by the strong band of the carboxylic acid v(O-H) Stretch form 2500-3030cm^{-1}. The signals of the Keggin stretching can still be observed for *v*(P-O) at 934.64cm and *v*(W-O_d-W) at 678.67.cm^{-1}. This also shows that the Keggin structure was still intact even after the reaction.

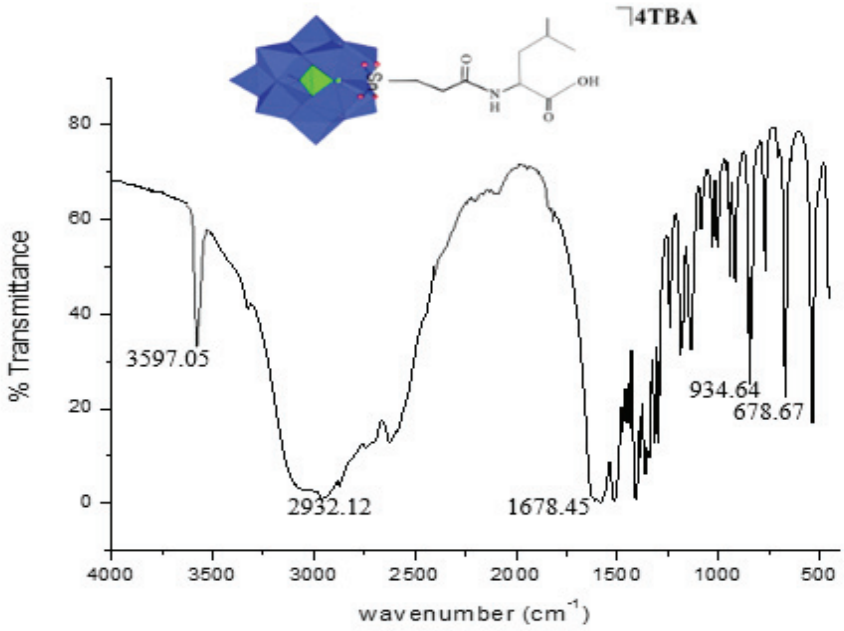

Figure 4.10. The FT-IR of TBA [K_{Sn}CO-Leu]

The thermogravimetric analysis experiment of TBA [K_{Sn}CO-Leu] was performed under nitrogen gas atmosphere with a heating rate of 10 °C·min^{-1} in the temperature range from room temperature to 1000 °C. As shown in Figure 4.11, the TGA curves has two main steps of the weight loss for both the organic moeities and the POM cluster. With increasing temperature there was the first sudden weight loss step from 300 to 360 °C with the weight loss of 12.56% is corresponding to the removal of leucine and the organotin moiety. The second weight loss steps of 55.10% in the range of 360–600 °C can be ascribed to the loss of all the remaining organic parts and complete decomposition of the Keggin cluster [$PW_{11}O_{39}$] residues in the compound.

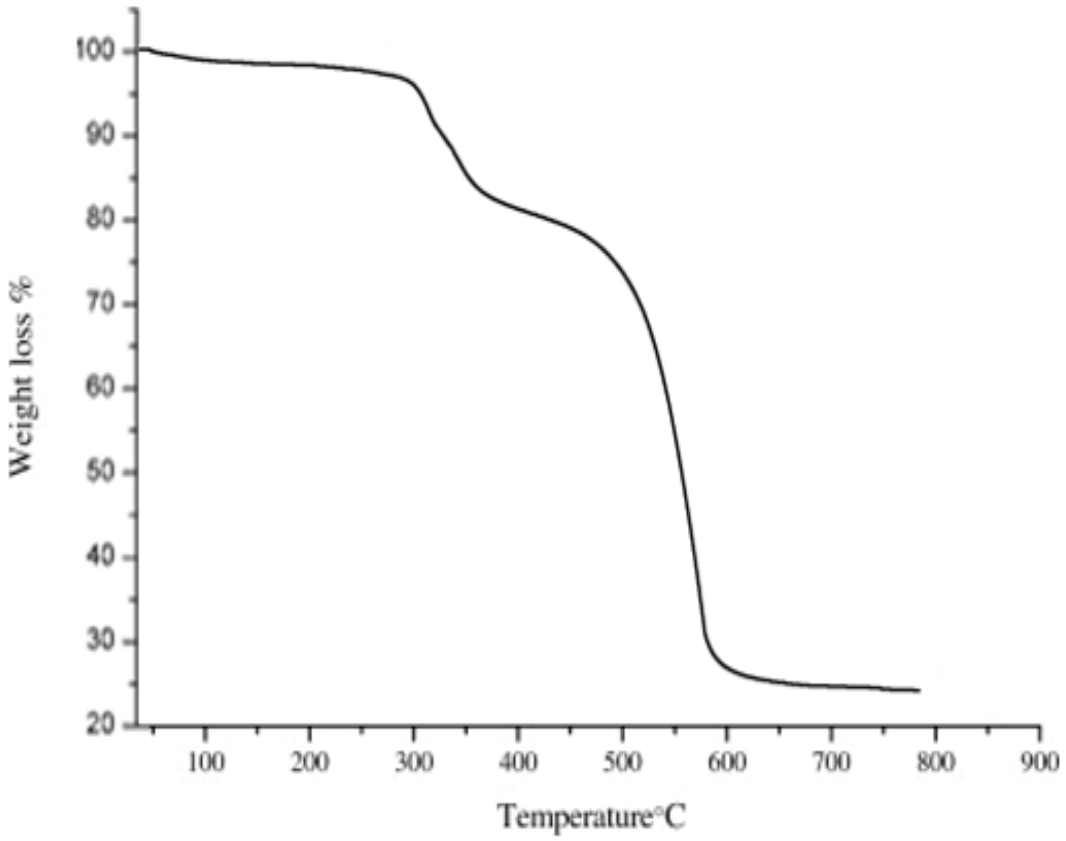

Figure 4.11. The TGA curve of TBA [K_{Sn}CO-Leu]

The Table 2.3 shows the two step weight losses of the whole decomposition of TBA [K_{Sn}CO-Leu]. The TG analyses results of the compound are in consistence with the calculated values. This also support the chemical composition of the successful synthesis of the compound.

Table 2.3: The TGA weight losses with temperature of TBA [K_{Sn}CO-Leu]

Residue	Temperature (°C)	Actual Weight loss (%)	Theoretical Weight Loss (%)
Organotin/Leucine	300 – 350	12.56	11.33
$TBA^{4+}/[PW_{11}O_{39}]^{7-}$	350 - 510	55.10	58.89
WO_3	> 600		

To observe the purity of the TBA [K_{Sn}CO-Leu] compound, the Powder XRD was implemented. As shown in Figure 4.12, the patterns measured for the synthesized compound indicated the phase purities of the compounds with the clear baseline.

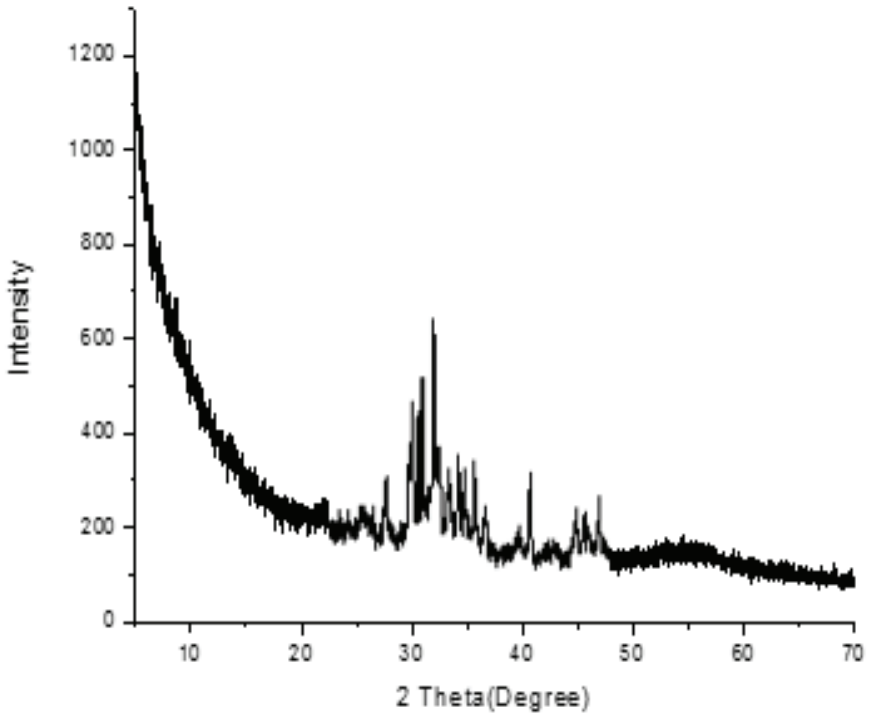

Figure 4.12. The obtained Powder XRD of TBA [K_{Sn}CO-Leu]

4.2. Lindqvist POM-BODIPY Hybrid

The Lindqvist POM was prepared following the reported literature procedure (Jim 2010). Nitric acid was used to oxidized the sodium tungstate ($Na_2WO_4.2H_2O$) dissolved in DMF at 40°C. The white solid product obtained after washing with diethyl ether was confirmed to be $Na_2W_6O_{19}$ (equation 3.5).

The SEM results (Figure 4.9) shows the morphology of the clearly formed crystals of the Lindqvist POM $[W_6O_{16}]^{2-}$

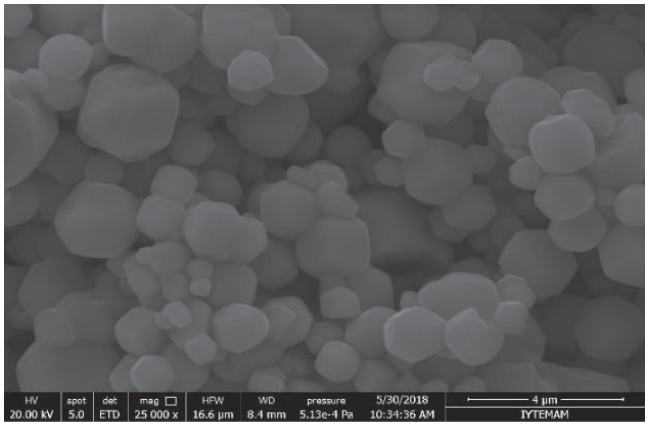

Figure 4.13. The SEM of crystals of $Na_2W_6O_{19}$

The EDX results shown in Table 4.4 gave the following Percent weights in which Na = 4.26%, W = 74.32% and O = 21.42% which corresponds with the theoretical value of 3.16% Na, 75.93% W and 20.91% O respectively.

Table 4.4: The EDX results of $Na_2W_6O_{19}$

Element	Weight%	Atomic %
Na	4.26	5.90
O	21.42	78.45
W	74.32	15.65
Total:	100.00	100.00

Following the FT-IR spectrum shown in Figure 4.14 has major stretching vibrations of $[W_6O_{19}]^{2-}$. It has low 1012.30cm^{-1}, strong sharp 987.89cm^{-1} and strong broad 673.45cm^{-1} for ν(W-O), ν(W–O_b–W) and ν(W–O_c–W) respectively. The vibration peaks from 1400cm^{-1} can be attributed to the water absorbed by the samples. There is resemblance in major stretching vibrations with the spectrum found in literature (Wu 2010)

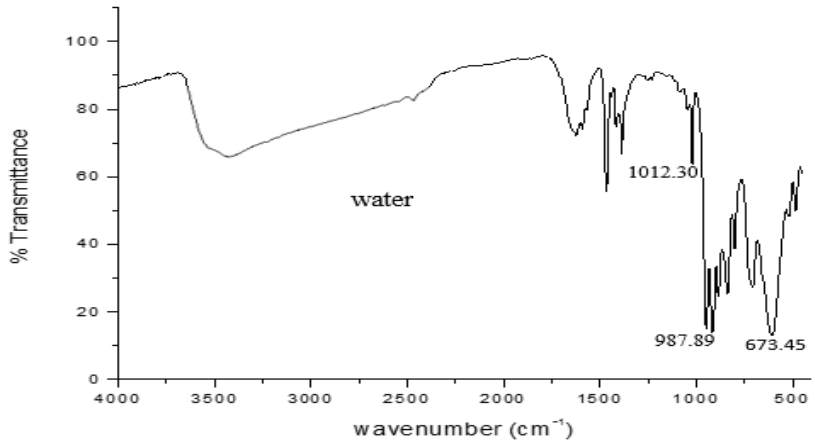

Figure 4.14. The FT-IR spectrum of the Lindqvist POM $[W_6O_{19}]$

To check the purity of the synthesized POM, the X-ray powder diffractions of compounds was carried out at room temperature with the angle in the range of up to 70°. The powder X-ray diffraction pattern (Figure 4.15) of the synthesized POM $[W_6O_{16}]^{-2}$ in showed a clear baseline.

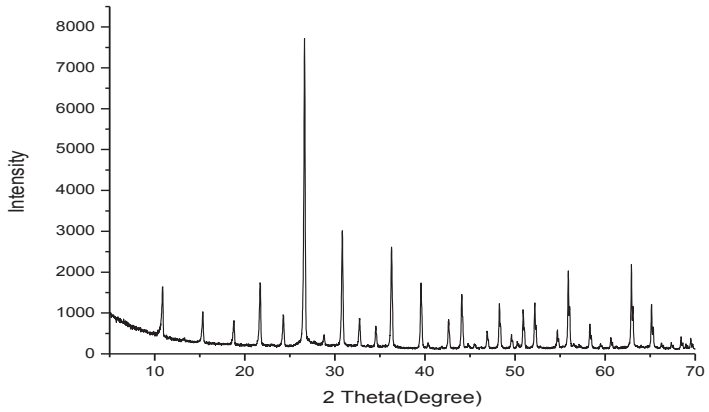

Figure 4.15. Powder XRD of $Na_2W_6O_{19}$

In the second step as shown in equation 3.6, the POM clusters was reacted with phosphine based BODIPY derivative dye which gave a brown solid product. The IR Spectrum (Figure 4.) show the similarity absorptions peaks in the POM cluster, dye and the product formed.

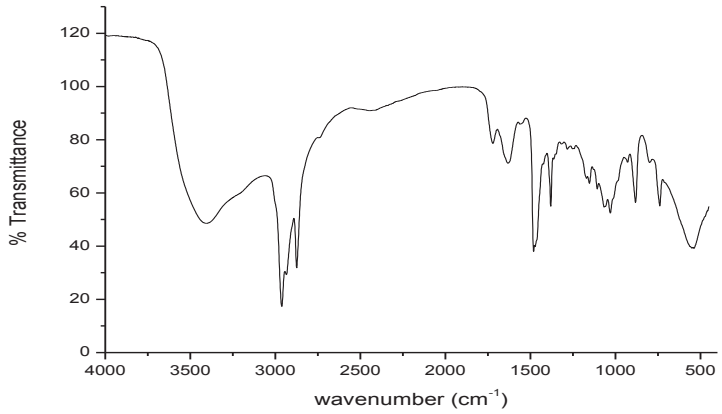

Figure 4.16. The IR spectrum of Lindqvist POM-Dye hybrid.

The characteristics IR peaks (Table 4.5) shows the intact Lindqvist POM in the region from 700cm^{-1} to 1000cm^{-1}. The other peaks above 1000cm^{-1} were deduced to be coming from the organic moiety.

Table 4.5: The characteristic IR peaks spectrum of: $Na_2W_6O_{19}$, dye and POM-Dye

Wave number (cm^{-1})			**Vibration Mode**
$Na_2W_6O_{19}$	**Dye**	**Product**	
–	2906, 2863	2929, 2832	ν (C-H)
–	1666, 1629	1737, 1691	ν (C-P)
–	1575, 1506	1460, 1346	ν (C-N)
985	–	1012	ν (W-O_t)
889	–	891	ν (W–O_b–W)
793	–	806	ν (W–O_c–W)

The thermogravimetric analysis of the synthesized hybrid compound given in Figure 4.17 exhibits three notable step mass losses in the temperature range from room temperature to 750 °C. The thermal stability of this hybrid was investigated under the atmosphere of N_2 with a heating rate of 10°C /min.

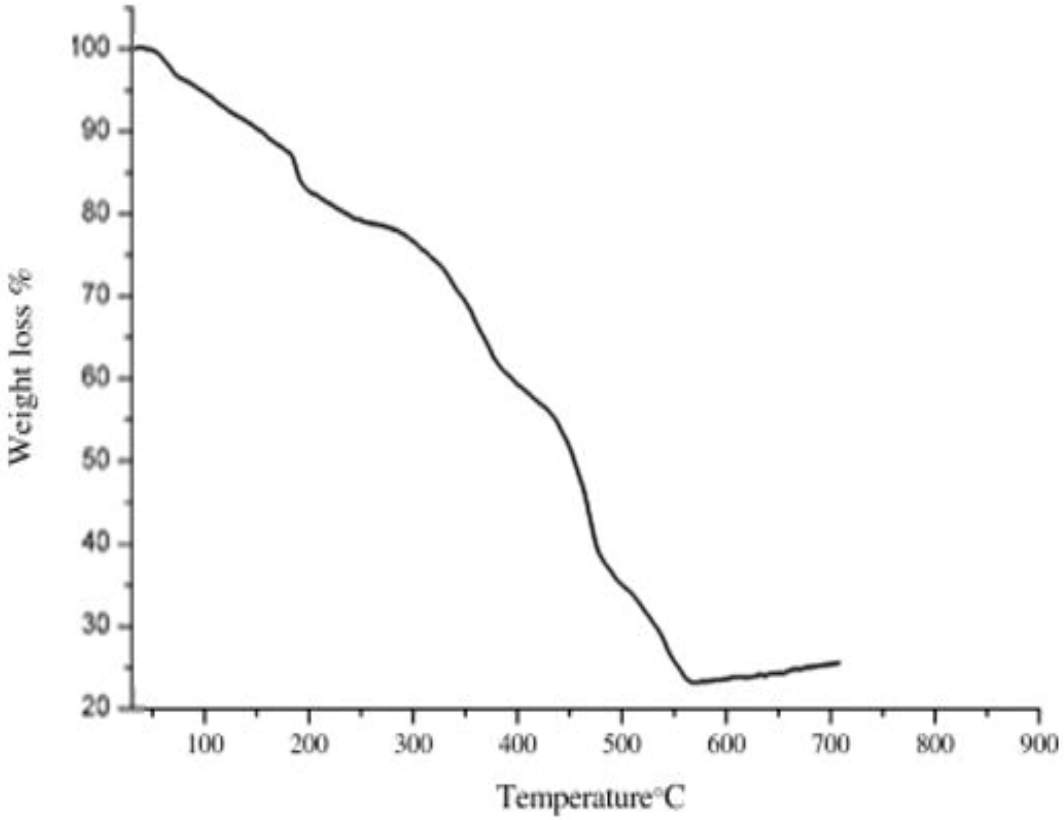

Figure 4.17. The TGA Curve of the Lindqvist POM-BODIPY hybrid

Table4.6 gives the overview of the residue weight losses were compared to the theoretically calculated masses of each of the residue in the compound. The small mass loss under 200°C can be attributed by the water molecules absorbed by the compound. The 49.64% weight loss is of the organic residues with a wide temperature range of 190-600°C corresponding with that for BODIPY derivative (Calc-48.89%). The last step from temperatures above 600°C shows the remaining of the POM (WO_3) residues (Calc-52.72%). The weight losses have well corresponded wıth the calculated weight loss. This also gives strong evidence to shows that the Lindqvist POM-BODIPY hybrid was successfully synthesized.

Table 4.6: The weight loss with temperature of Lindqvist POM-BODIPY hybrid

Residue	**Temperature (°C)**	**Actual Weight loss (%)**	**Theoretical Weight Loss (%)**
water	< 200	9.47	0.00
organic	200 - 600	49.64	48.89
WO_3	> 600	0.12	52.72

Powder XRD measurements caried out in of the hybrid shown in Figure 4.18, exhibits the diffraction peaks with a clear baseline. This indicates that the powders of the products are pure and in single phases.

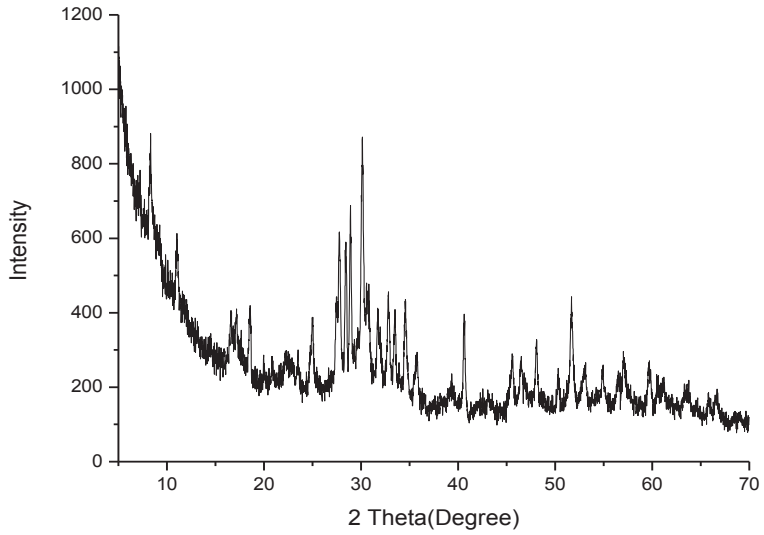

Figure 4.18**.** Powder XRD of Lindqvist POM-BODIPY dye hybrid

CHAPTER 5

CONCLUSION

The inorganic-organic hybrid materials containing Polyoxotungstatess with organic units were suucessfully synthesized. This was done by use of an organo-tin groups grafted in the lacunary Keggin POM which enabled it to be covalent attached with an organic ligands by amidation reaction. The Lindgvist POM self assembled with the phosphine based BODIPY derivative by hydrothermal method and the fluorescent properties investigation of the hybrid formed was carried out. The final synthesized compounds were characterised by FT-IR, PXRD and TGA

The $TBA_4[PW_{11}O_{39}SnCH_2CH_2COOH]$ was successfully synthesized following the literature procedure to be used for obtaining organo-tin groups. This enabled to undergoe amidation reactions with amine group containing organic compounds. Leucine and 3-Amino Phenol were the organic compounds combine with which gave good yields of amide compounds denoted as TBA $[K_{Sn}CO\text{-}Leu]$ and TBA $[K_{Sn}CO\text{-}Ph]$ respectively. The appearance of the of the amide bond characteristics gave enough strong evidence for the formation of the amide compound $TBA_4[PW_{11}O_{39}SnCH_2CH_2CONHR]$.

Secondly the Lindqvist POM $[W_6O_{19}]^{2-}$ successfully self assembled with the phosphine based based BODIPY unit in good yields. The final hybrid formed did not show any flourescence as the uncombined BODIPY unit. Therefore it can be deduced that the POM made the BODIPY unity to loose its fluorescence properties.

Future work researches are needed in which these two important compounds in chemistry and material science in POMs and BODIPY with wide applications can be combined. Furthermore finding suitable applications of hybrids made from these componds can be achieved. The improved properties of these inorganic-organic hybrids attained from these two compounds can be of great beneficial to science.

REFERENCES

Anthony R. West. 2015. *Solid State Chemistry and Its Applications*. 2nd Edition, John Wiley & Sons: England.

Burgess k, Loudet A. 2007. *BODIPY Dyes and Their Derivatives: Syntheses and Spectroscopic Properties.* Texas A & M University, USA. Chemical Review.

Canturk C. 2015. *The design and synthesis of fluorescent chemosensor for the detection of Gold and Mercury metal species*. M.S.Thesis, İzmir Institute of Technology, Turkey.

Cronin L. Et al. 2010. *Polyoxometalates: Building Blocks for Functional Nanoscale Systems.* Reviews. Wiley-VCH Verlag GmbH & Co. KGaA, Weinheim. The University of Glasgow, UK.

Byrappa, K. 2013. *Handbook of Hydrothermal Technology.* 2nd Edition. William Andrew: New York.

Eanes M, et al. 2015. *Hydrothermal synthesis and characterization of one dimensional chain structures of monolacunary Keggin polyoxoanions substituted with copper.* Inorganica Chimica Acta, Elsevier. İzmir Institute of Technology, Turkey.

Eanes M; Onen B. 2014**.** *Hydrothermal synthesis and characterization of a novel supramolecular hybrid based on Keggin and Cu(I) complex*. Inorganic Chemistry Communications, Elsevier. İzmir Institute of Technology, Turkey.

Ece Özlem. 2012. *Hydrothermal synthesis and structural characterization of open-framework metal phosphates templated with organic diamines*. M.S.Thesis, İzmir Institute of Technology, Turkey.

Eral, L. 2006. *Hydrothermal synthesis and characterization of transition metal (Mn and V) oxides containing phosphates*. MSc thesis, İzmir Institute of Technology, Turkey.

Fatma Hmida et al. 2017. *Hydrothermal synthesis and characterization of two novel inorganic-organic hybrid materials based on polyoxotungstate clusters.* Journal of Molecular Structure.

Frontera Antonio, et al. 2015. *Tuning the topology of hybrid inorganic–organic materials based on the study of flexible ligands and negative charge of polyoxometalates.* Coordination Chemistry Reviews, Elsevier. University of Belears, Spain.

Frontera Antonio. Et al. 2014. *Recent developments in the crystal engineering of diverse coordination modes (0–12) for Keggin-type polyoxometalates in*

hybrid inorganic–organic architectures. Coordination Chemistry Reviews, Elsevier. University of Belears, Spain.

Guo, J. et al. 2013. *Two new polyoxometalate-templated supramolecular compounds constructed by a new tridentate ligand 2,4,6-tris[1-(4-oxidroxypyridinium)-ylmethyl]-mesitylene.* Inorganic Chimica Acta, Elsevier. Northeast Normal University, Changchun, China

Hagrman, P. J et al. 2001. *Molecular Manipulation of Solid State Structure: Influences of Organic Components on Vanadium Oxide Architectures.* Solid State Sciences.

Hasenknopf Bernold, et al. 2007. *A general strategy for litigation of organic and biological molecules to Dawson and Keggin polyoxometalate*. Organic letters. University of Paris, Paris, France

Hasenknopf Bernold, et al. 2013. *Post functionalization of Keggin silicotungstates by general procedures.* Polyhedron, Elsevier. University of Paris, Paris, France

Hasenknopf Bernold, et al. 2013. *Regioselective double organic Functionalization of Polyoxotungstates through Electrophilic addition of isocyanates*. European journal of inorganic chemistry. University of Paris, Paris, France

Jin Bakaong, et al. 2010. *Organic/polyoxometalate hybridization dyes: Crystal structure and enhanced two-photon absorption.* Dyes and Pigments, Elsevier. Nanjing University, Nanjing, China.

Joseph Lakowicz. 1999. *Principles of Fluorescence Spectroscopy*, Kluwer Academic/Plenum Publishers.

Keeler James. 2010. *Understanding NMR Spectroscopy.* 2nd edition. Wiley. pp. 184–187.

Lambert .C. et al. 2016 *Metal-organic frameworks: structure, properties, methods of synthesis and characterization*, Southern Federal University, Russia. Russian Chemical Reviews 85.

Matt Benjamin, et al. 2011. *Elegant approach to the synthesis of an Unique heteroleptic cyclometalated iridium (iii)-polyoxometalate conjugate*. Organometallics. J.A.C.S. University of Pierre and Marie Curie, Paris, France.

Matt Benjamin, et al. 2011. *Elaboration of covalently linked polyoxometalates with ruthethenium and pyrene chromophores and characterization of their physical properties*. Inorganic chemistry, J.A.C.S. University of Pierre and Marie Curie, Paris, France.

Meliane Pierre, et al. 2015. *A high fatigue resistant, photoswitchable fluorescent spiropyran–polyoxometalate–BODIPY single-molecule.* Royal society of chemistry. University of Versailles, Versailles, France.

Meliane Pierre, et al. 2017. *Photochromism and Dual-Color Fluorescence in a Polyoxomet alate–Benzospiropyran Molecular Switch.* Wiley-VCH Verlag GmbH & Co. KGaA, Weinheim.

Meliane Pierre, et al. 2010. *Hybrid Organic-Inorganic Polyoxometalate Compounds: From Structural Diversity to Applications.* J.A.C.S. University of Versailles, Versailles, France.

Neves C. S. 2014. *Development of fluorescent silica nanoparticles organic and inorganic fluorophores: synthesis and characterization.* PhD. Thesis, University of Porto. Portugal.

Odobel Fabrice, et al. 2009. *Coupled Sensitizer-catalyst dyads: Electron-transfer Reactions in a Perlyne-Polyoxometalate conjugate.* Chemistry A European Journal. University of Nantes. Nantes, France.

Önen Banu. 2011. *Hydrothermal synthesis and characterization of vanadium and tungsten oxide containing organic-inorganic hybrid material*. M.S.Thesis, İzmir Institute of Technology, Turkey.

Proust A et al. 2012. *Functionalization and post-functionalization: a step towards polyoxometalate-based materials.* Review. Chemical society. University of Pierre and Marie Curie, Paris, France.

Proust A. et al. 2008. *Functionalization of polyoxometalates: towards advanced applications in catalysis and materials science.* The Royal Society of Chemistry. University of Pierre and Marie Curie, Paris, France.

Riyadh Alshammari. 2014. *Hydrothermal synthesis of organically-linked polyoxometalates.* M.S. Thesis, Clemson University. USA.

Santoni Marie Pierre, et al. 2014. *Covalent multi-component systems of polyoxometalates and metal complexes: Toward multi-functional organic–inorganic hybrids in molecular and material sciences*. Coordination Chemistry Reviews, Elsevier. University of Montreal, Montreal, Canada.

Rompel A, et al. 2018. *Synthesis, structures and applications of electron-rich polyoxometalates.* Nature reviews Chemistry. Donetsk National University, Vinnytsia, Ukraine.

Sanchez C, et al. 2001. *Designed Hybrid Organic-Inorganic Nanocomposites from Functional Nano-building Blocks.* Reviews, J.A.C.S. University of Pierre and Marie Curie, Paris, France.

Sankar Sib Mal. 2008. *Synthesis, Structure and Properties Transition Metal of Multi Metal-Substituted Polyoxotungstates*. PhD. Thesis. Jacobs University. Germany.

Schubert, U. 2000**.** *Synthesis of Inorganic Materials,* 2nd edition. Wiley-VCH: Weinheim.

Shan Wenpeng. 2014. *Molecular shape amphiphilic based on Keggin polyoxometalates and iso-butyl polyhedral oligomeric silsesquioxanes: synthesis and characterization*. MSc Thesis. University of Akron, Ohio, USA.

Skoog, D, A and West, D, M. 2007. *Principles of Instrumental Analysis*, 2nd edition. Saunders College, Philadelphia.

Solomon T. W. et al. 2014. *Organic Chemistry*, 9th Edition. John Wiley & Sons Inc, Philadelphia, USA. P. 246 – 289.

Song Yu-Fei, et al. 2018. *Synthesis, structural characterization and fluorescence enhancement of chromophore-modified polyoxometalates.* Polyoxometalates. Structural Chemistry. Beijing University of Technology, Beijing, China.

Tsunashima R, & Yu-Fei Song. 2012. *Recent advances on polyoxometalate-based molecular and composite materials.* Critical review, The Royal Society of Chemistry. Yamaguchi University, Japan.

Wang Qian, et al. 2017. *Synthesis and Properties of a New Organic-Inorganic Hybrid Compound Based on α-Keggin polyoxometalate: $[Cu(Dione)_2(H_2O)]_2(SiW_{12}O_{40})$*. Xinyang College, Henan. China.

Wen-Bin Yang. Et al. 2015. *Photocatalytic properties of two POM-templated organic–inorganic hybrid compounds.* Inorganic Chemistry Communications, Elsevier. University of Chinese Academy of Science, China.

Yang Chu. 2017**.** *Rational controlled self-assembly behavior of inorganic-organic hybrids in solution.* PhD. Thesis. University of Akron. Germany.

Yang Guo. et al. 2016**.** *A New 2-D Inorganic–Organic Hybrid Polyoxometalate Based on Mono-Cu-Substituted $[CuSiW_{11}O_{39}]_n^{6n}$ Chains and $[Cu(en)_2]^{2+}$ Bridges.* Springer. Fuzhou University, Fujian. China.

Yan-Kun Li, et al. 2017. *A survey of the influence of EEDQ on efficient Post-functionalization of an Anderson-type polyoxomolybdate towards construction of inorganic-organic hybrids.* Elsevier. North University of China, Shanxi, China.

Zhang Jiangwei, et al 2017. *Recent advances in alkoxylation chemistry of polyoxometalates: From synthetic strategies, structural overviews to functional applications.* Coordination Chemistry Reviews, Elsevier. Tsinghua University, Beijing, China.